Quaternary Science Reviews 31 (2012) 93–111

Contents lists available at SciVerse ScienceDirect

Quaternary Science Reviews

journal homepage: www.elsevier.com/locate/quascirev

Holocene glacial and climate history of Prince Gustav Channel, northeastern Antarctic Peninsula

Mieke Sterken [a,1], Stephen J. Roberts [b,1], Dominic A. Hodgson [b,1,*], Wim Vyverman [a], Andrea L. Balbo [b,2], Koen Sabbe [a], Steven G. Moreton [c], Elie Verleyen [a]

[a] Laboratory of Protistology and Aquatic Ecology, Biology Department, Ghent University, Krijgslaan 281-S8, B-9000 Gent, Belgium
[b] British Antarctic Survey, Natural Environment Research Council, High Cross, Madingley Road, Cambridge CB3 0ET, UK
[c] Natural Environment Research Council Radiocarbon Facility, Scottish Enterprise Technology Park, East Kilbride, G75 0QF, UK

ARTICLE INFO

Article history:
Received 25 October 2010
Received in revised form
26 October 2011
Accepted 31 October 2011
Available online 12 December 2011

Keywords:
Antarctic Peninsula
Deglaciation
Climate change
Palaeoclimate
Marine
Terrestrial

ABSTRACT

The Antarctic Peninsula is one of the most rapidly warming regions on Earth, as evidenced by a recent increase in the intensity and duration of summer melting, the recession of glaciers and the retreat and collapse of ice shelves. Despite this, only a limited number of well-dated near shore marine and lake sediment based palaeoenvironmental records exist from this region; so our understanding of the longer-term context of this rapid climate change is limited. Here we provide new well-dated constraints on the deglaciation history, and changes in sea ice and climate based on analyses of sedimentological proxies, diatoms and fossil pigments in a sediment core collected from an isolation basin on Beak Island in Prince Gustav Channel, NE Antarctic Peninsula (63°36′S, 57°20′W). Twenty two radiocarbon dates provided a chronology for the core including a minimum modelled age for deglaciation of 10,602 cal yr BP, following the onset of marine sedimentation. Conditions remained cold and perennial sea ice persisted in this part of Prince Gustav Channel until c. 9372 cal yr BP. This was followed by a seasonally open marine environment until at least 6988 cal yr BP, corresponding with the early retreat and disintegration of the ice shelf in southern Prince Gustav Channel. Following isolation of the basin from 6988 cal yr BP a relatively cold climate persisted until 3169 cal yr BP. A Mid-late Holocene climate optimum occurred between 3169 and 2120 cal yr BP, inferred from multiple indicators of increased biological production. This postdates the onset of the Mid-late Holocene climate optimum in the South Shetland Islands (4380 cal yr BP) and the South Orkney Islands (3800 cal yr BP) suggesting that cooler climate systems of the Weddell Sea Gyre to the east of the Peninsula may have buffered the onset of warming. Climate deterioration is inferred from c. 2120 cal yr BP until 543 cal yr BP. This was followed by warming. Superimposed on this warming trend, the instrumental record of recent warming at nearby Hope Bay is mirrored by a recent increase in the lake's primary production and a shift in the diatom communities in the uppermost 3 cm of sediments, suggesting that this is amongst the first records to show an ecological response to recent rapid temperature increase. These new constraints on glaciological and climate events in Prince Gustav Channel are reviewed in the context of wider changes in the Antarctic region.

1. Introduction

The Antarctic Peninsula (AP) is particularly sensitive to climate change. Currently it is one of the most rapidly warming regions on Earth, with temperatures rising at six times the global mean (0.6 ± 0.2 °C) during the 20th century (Houghton et al., 2001; Vaughan et al., 2003). This warming has resulted in an acceleration in the intensity and duration of summer melting by up to 74% since 1950 (Vaughan, 2006), the recession of snowfields and glaciers (Cook et al., 2005), and a reduction in the duration of sea ice cover (Parkinson, 2002). It has also been linked to the retreat and collapse of ice shelves (e.g., Vaughan and Doake, 1996; Rott et al., 1998; Scambos et al., 2003; Hodgson, 2011) causing increased flow velocities of their feeder glaciers (De Angelis and Skvarca, 2003; Scambos et al., 2004).

In order to better understand the longer-term context of these anomalies, ice, marine, and lake sediment cores, together with geomorphological evidence, are being used to reconstruct palaeoenvironmental changes through the Holocene. To date, most ice

* Corresponding author. Tel.: +44 1223 221635.
E-mail addresses: mksterken@gmail.com (M. Sterken), sjro@bas.ac.uk (S.J. Roberts), daho@bas.ac.uk (D.A. Hodgson), Wim.Vyverman@ugent.be (W. Vyverman), balbo@imf.csic.es (A.L. Balbo), Koen.Sabbe@ugent.be (K. Sabbe), S.Moreton@nercrcl.gla.ac.uk (S.G. Moreton), Elie.Verleyen@ugent.be (E. Verleyen).
[1] These authors contributed equally to this research.
[2] Present address: Institució Milà i Fontanals – Consejo Superior de Investigaciones Científicas (IMF-CSIC), C/Egipcíaques 15, 08001 Barcelona, Spain.

0277-3791/$ – see front matter © 2011 Elsevier Ltd. All rights reserved.
doi:10.1016/j.quascirev.2011.10.017

cores from the AP region only span a few thousand years, although a new ice core extracted from James Ross Island is predicted to span the late glacial and Holocene (Mulvaney et al., 2007). Therefore, investigations of the deglaciation of the Antarctic Peninsula Ice Sheet from its Last Glacial Maximum (LGM) limits, and the regional Holocene climate evolution have largely been derived from marine sediment cores, for example in Marguerite Bay (Ó Cofaigh et al., 2005), Lallemand Fjord (Taylor et al., 2001), Bismark Strait (e.g., Domack, 2002) and Bransfield Strait (e.g., Barcena et al., 1998). On land, records have been derived from lake sediment cores, for example from Alexander Island (e.g., Bentley et al., 2005; Smith et al., 2007; Roberts et al., 2008), Horseshoe Island (Wasell and Håkansson, 1992), the western and northern islands of the Antarctic Peninsula (e.g., the South Shetland Islands; Björck et al., 1993), James Ross Island (e.g., Björck et al., 1996), and the South Orkney Islands (Jones et al., 2000; Hodgson and Convey, 2005). Well-dated terrestrial and near shore marine records spanning the entire Holocene are however still rare, particularly along the northeastern margin of the AP, the Weddell Sea margin, and the western margin of the AP between the South Shetland Islands and Marguerite Bay (Bentley et al., 2009; Hodgson et al., 2009).

Although the deglaciation of the Antarctic Peninsula Ice Sheet since the LGM, and Holocene environmental and climate changes are poorly constrained in some areas, attempts have been made to formulate a regional consensus (e.g., Hjort et al., 2003; Ingólfsson et al., 2003; Bentley et al., 2009; Hodgson et al., 2009). However, the limited number of records from the AP means that there are still considerable gaps in understanding, for example of the differences in the climate and glaciological history of the east vs. the western margin of the AP, and between the AP and other regions of Antarctica.

In this paper, we analyse the record of palaeoenvironmental change from sediments that have accumulated in an isolation basin on Beak Island in northern Prince Gustav Channel (Figs. 1 and 2). We integrate a radiocarbon dated stratigraphy, sedimentological, fossil diatom and pigment analyses to reconstruct and constrain the timing of the main glaciological and palaeoclimate events occurring there during the Holocene.

2. Site description

Beak Island (63°36′S, 57°20′W) is a partially emerged periphery of an inactive volcanic caldera situated in Prince Gustav Channel between Vega Island and the Tabarin Peninsula (Figs. 1 and 2a). The island is composed of Miocene volcanic rocks, mainly porphyritic basalt, hyaloclastites and pillow lavas, belonging to the James Ross Island Volcanic group (Bibby, 1966). Beak Island is currently free of permanent snow fields, ice caps or glaciers, and is assumed to have a similar continental climate regime to the Tabarin Peninsula (28 km to the northeast) where mean annual temperatures are −5.3 °C and mean annual precipitation 60.53 mm (Data from Base Esperanza, Hope Bay). The regional climate is influenced by (1) the westerly storm tracks bringing humid, warm air from the northwest, and by (2) the cold barrier winds bringing arid air-masses from the south and southwest (i.e., the Weddell Sea) (Björck et al., 1996). The region is influenced by the rain shadow effect of the mountains of the Antarctic Peninsula. Snowfall periodically occurs during summer, followed by rapid melting and long dry periods.

Several lakes and ponds occur on the island (Fig. 2a, b). Beak Lake 1 (63°36′38″S, 57°20′20″W, the name is unofficial) is the largest and deepest lake (c. 24 m), it is near circular, with a diameter of c. 400 m and occupies a depression created by a secondary eruption vent. The current retaining sill height is 10.95 ± 10 cm above the present high tide mark and is lower than the 14.91 ± 10 cm m a.s.l. Holocene marine limit (Fig. 2a; Roberts et al. 2011). The lake is flanked by a >10 m rock cliff 200 m to the west and northwest, and is bordered by periglacially patterned ground to the north, east and south. Moss banks occur on the north-western shores of the lake, and are dissected by a series of small, braided meltwater streams emanating from a snow bank on the adjacent slope (Fig. 2b). Beak Lake 1 has a single outflow to the southwest, which discharges to the sea via a series of ponds and raised shorelines. The outflow is vegetated by thick orange and green microbial mats and was nearly inactive at the time of sampling (January 2006). Ice cover is likely to persist for 8–9 months per year.

3. Methods

3.1. Lake sediment coring

Following routine limnological measurements (cf. Hodgson et al., 2001), core sites were selected on the basis of bathymetric mapping with a hand-held echo sounder along static lines. Sediment cores were collected at 20 m water depth using a Livingstone corer (Wright, 1967). One core sequence (sections BK 1E and BK 1D) was sectioned at 0.5 cm resolution in the field, sealed in sterile Whirlpack bags and stored frozen; a duplicate core (BK1G) was retained intact for high resolution, non-destructive core scanning.

3.2. Geochronology

A chronology for the sediment sequence was established by AMS radiocarbon (^{14}C) dating of macrofossils of the aquatic moss *Cratoneuropsis Chilensis* (also referred to as *Cratoneuropsis relaxe subsp. minor*) (Ochyra, 2008, Ochyra pers. comm.), and macrofossils of lacustrine cyanobacteria. Bulk (inorganic) sediments were dated in 7 samples where no macrofossils were present. Paired cyanobacterial mat and moss macrofossils were analysed at 15.5–16 cm, and overlaps between core sections were independently dated at 73–74 cm.

Macrofossils were hand-picked from frozen bulk material, after overnight defrosting at 5 °C, immersed in ultra-pure (18.2 m Ohm) water, sealed and placed in an ultrasonic bath for an hour and then refrozen and stored. Samples were sent frozen to the Scottish Universities Environmental Research Centre (SUERC) and Beta Analytic (Miami, Florida) for accelerator mass spectrometry (AMS) radiocarbon dating. SUERC-samples were heated in 2 M HCl (80 °C for 8 h), rinsed in deionised water, until all traces of acid had been removed, and dried in a vacuum oven. Inorganic sand and rock fragments in samples SUERC-12947, 12574, 12575, 12576, 12577 were removed by sieving/hand-picking and set aside from finer organic bearing material before combustion. Moss samples dated by Beta Analytic (BETA 288864-67) were leached with a 0.5M–1.0M HCl bath to remove carbonates, heated to 70 °C for 4 h. Leaching was repeated until no carbonate remained, followed by rinsing to neutral 20 times with deionised water, then placed in 0.5%–2% solution of NaOH for 4 h at 70 °C and rinsed to neutral 20 times with deionised water. The process was repeated until no additional reaction (typically indicated by a colour change in the NaOH liquid) was observed. Samples were then leached again in a 0.5M–1.0M HCl bath to remove any CO_2 absorbed from the atmosphere by the NaOH soakings and to ensure initial carbonate removal was complete, and then dried at 70 °C in a gravity oven for 8–12 h.

Dates are reported, in years AD for 'modern' moss macrofossils, as conventional radiocarbon years BP (^{14}C yr BP) ± 1σ, and as calibrated years BP (cal yr BP relative to AD 1950). For the 'modern' radiocarbon samples calibration was carried out using CALIBomb with the SH1 compilation of Southern Hemisphere datasets (Hua and Barbetti, 2004; Reimer et al., 2004b). The remaining dates were calibrated in CALIB v6 (Reimer and Reimer, 2011) using the SHCal04 ^{14}C atmosphere dataset (McCormac et al., 2004; Reimer et al., 2004a) for freshwater samples, the MARINE09 calibration curve (Reimer et al., 2009) for marine samples, and a mixed MARINE09-SH04 curve (50% marine) for samples at the marine–lacustrine transition.

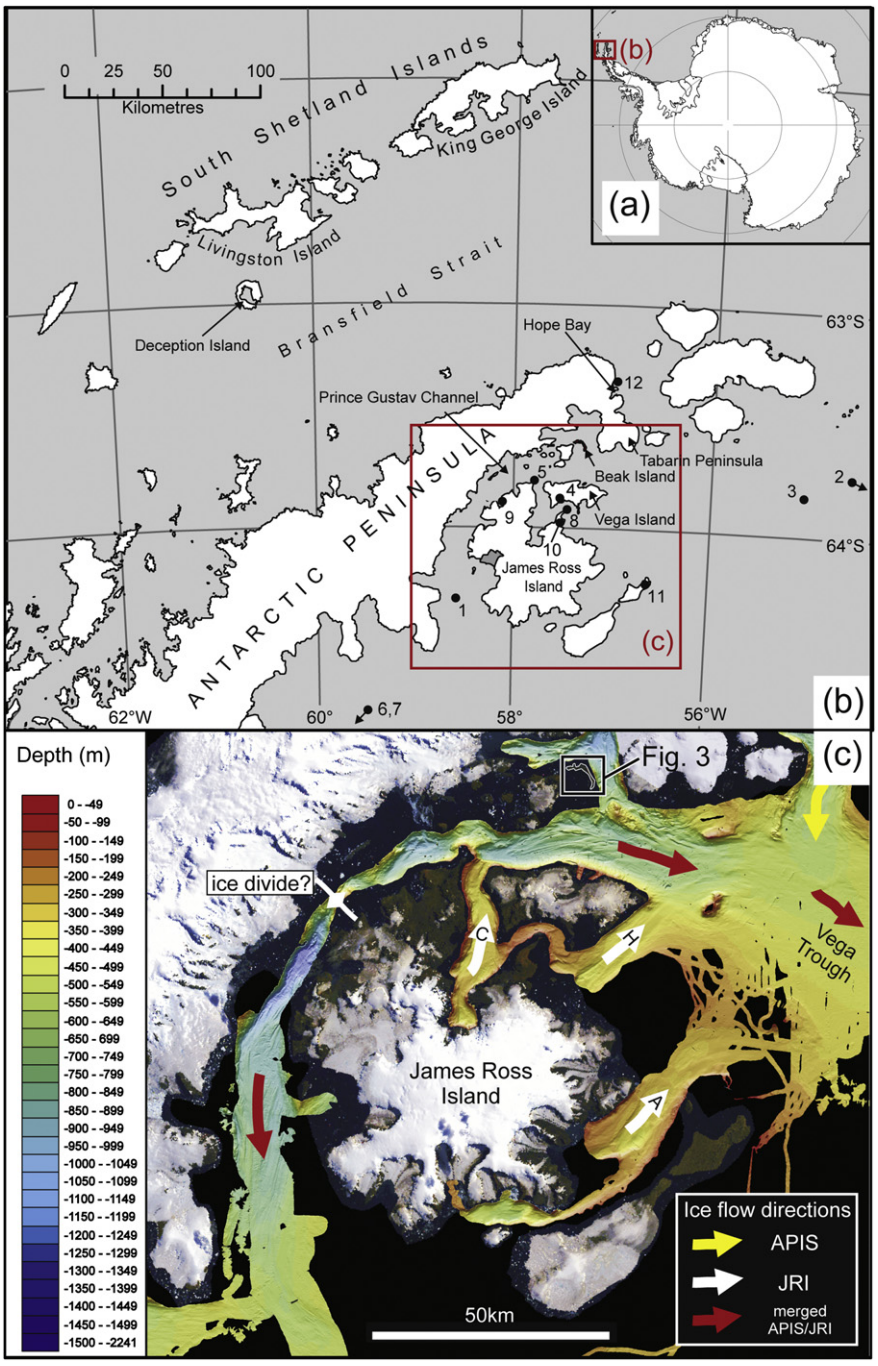

Fig. 1. Map of the northern Antarctic Peninsula region, showing Beak Island and locations mentioned in the text. Numbered sites with chronological constraints on deglaciation include (1) Southern Prince Gustav Channel, inferred maximum c. 16,700 ^{14}C yr BP (19,950 cal yr BP) (Pudsey et al., 2006); (2) Outer continental shelf in the NW Weddell Sea maximum of 20,319 cal yr BP (Smith et al., 2010); (3) continental shelf edge, 18,510 cal yr BP (Heroy and Anderson, 2007); (4) southwest Vega Island 11,911 cal yr BP (Zale and Karlén, 1989); (5) Cape Lachmann on James Ross Island 10,718 cal yr BP (Ingólfsson et al., 1992) and 8000 ± 800 yr BP at a higher altitude (Johnson et al. 2011); (6) inner shelf of the northwestern Weddell Sea 10605, 9569 and 8832 cal yr BP (Domack et al., 2005); (7) inner Larsen-A Ice Shelf region, 10,700 ± 500 yr BP (Brachfeld et al., 2003); (8) The Naze, James Ross Island, 8023–7512 cal yr BP (Ingólfsson et al., 1992, p. 213); (9) Brandy Bay c. 5510–5080 cal yr BP (Hjört et al., 23 1997, p. 271); (10) Terrapin Lake, 4645–3110 cal yr BP (Björck et al., 1996, p. 215); (11) Seymour Island 7500 ± 700 yr BP (Johnson et al. 2011); (12) Hope Bay, minimum extrapolated age of 6735–7471 cal yr BP (Zale, 1994b). Swath bathymetry data in Fig. 1c show the location of Beak Island in the context of a major former outlet of the Antarctic Peninsula Ice Sheet and ice flow directions of the former Antarctic Peninsula Ice Sheet and James Ross Island ice sheets (adapted and reproduced with permission from Johnson et al. (2011) which synthesises data from RVIB Nathaniel B Palmer cruises NBP0003 and NBP0107; RRS James Clark Ross cruise JR71; RVIB Nathaniel B Palmer cruises 0201, 0502 and 0602 and HMS Endurance surveys).

Absolute percentage of modern carbon (pMC) data were corrected according to $^{13}C/^{12}C$ isotopic ratios from measured pMC, where the "modern" (i.e., 1950) pMC value is 100 and the present day (2010) pMC value is 107.5. For the marine samples, dates were corrected for the Antarctic marine reservoir effect by using a ΔR value of 880 ± 50 years (1280 ± 50 minus the global marine reservoir of 400 years) based on the nearest measurements of the pre-1950 AD marine reservoir effect at the Hope Bay refuge which consists of penguin bones from animals consumed during the unplanned winter of Nordenskölds 1903 Expedition that have been dated at 1280 ± 50 ^{14}C yr BP (LU3101) (Björck et al., 1991b). 'Classical' age-depth modelling was undertaken using CLAM software (http://www.chrono.qub.ac.

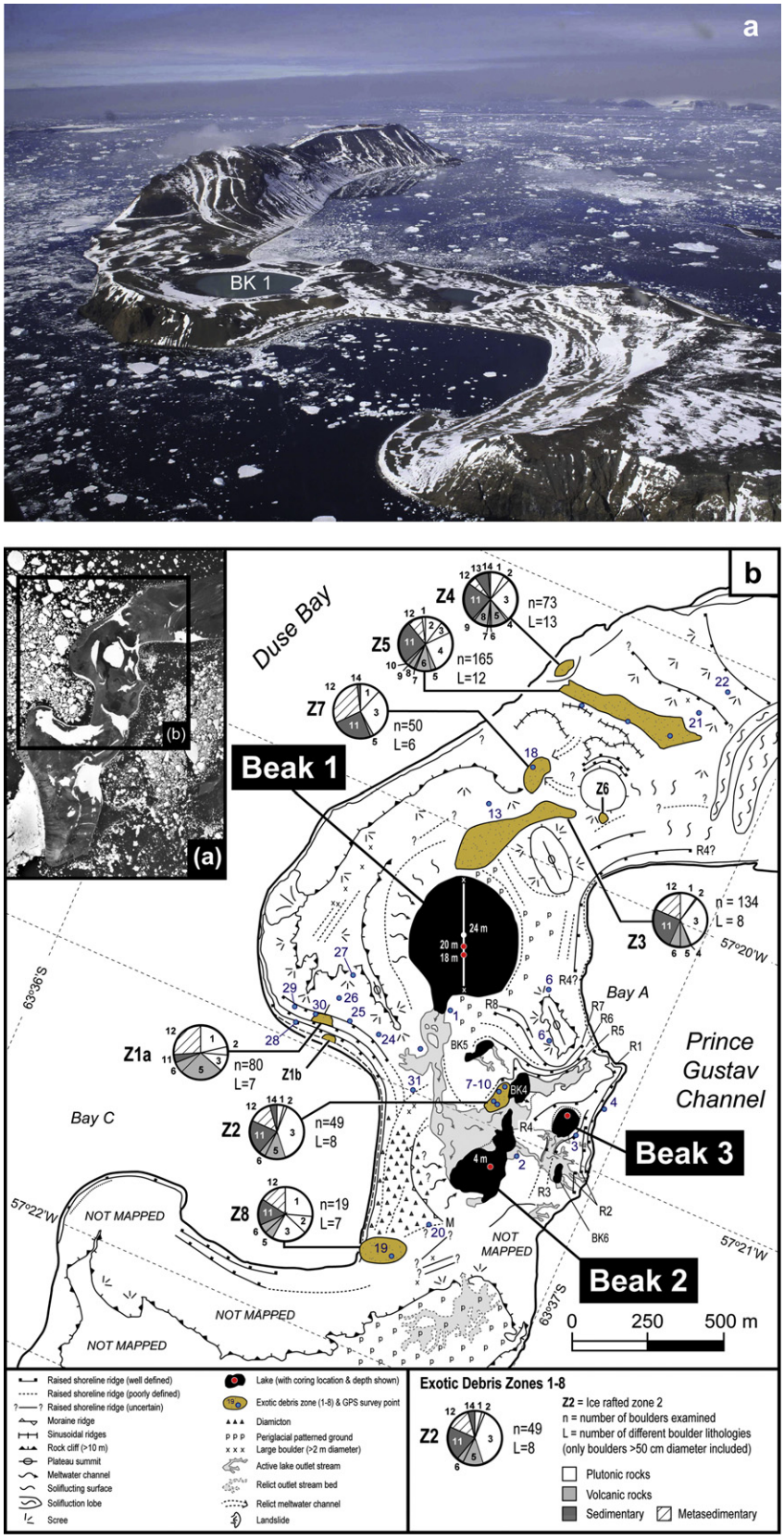

Fig. 2. (a) Oblique aerial view of Beak Island and Beak Lake 1 (BK 1) from the north (b) Geomorphological map of the central part of Beak Island showing the study site (Beak 1) and the position of the lake sediment core (20 m). Surveying was carried out using a Trimble 5700 GPS. Altitudes were referenced to vertical datum WGS84 and corrected using the EGM96 geoid model.

uk/blaauw/clam.html; (Blaauw, 2010)), with probability distributions for modern 'bomb'-carbon influenced, and mixed marine/freshwater samples generated and imported from OxCal v4 (www.c14.arch.ox.ac.uk/oxcal.html; Bronk Ramsey, 2001); all median calibrated ages and ranges quoted are 2σ error. Interpolated ages in the text are based on the 'best-fit' age from the CLAM age-depth model. To assist in future with tracking of reservoir correction and calibration procedures, ages cited in the text have not been rounded. Independent constraints on the Beak Lake 1 chronology were provided by comparing visible tephra layers in the core with the regional tephrochronology.

3.3. Stratigraphy and sedimentary properties

The cores were photographed, macroscopically described, and analysed for wet density, dry weight, organic content and carbonate composition following standard methods (Dean, 1974). Wet mass and volume specific magnetic susceptibility was measured using a Bartington 1 ml MS2G sensor. For C/N measurements, samples were dried, and carbonates removed by addition of 5% HCl then washed and wet sieved through 2 mm and 63 μm mesh, and vacuum filtered to remove the clay fraction (<4 μm). Samples were homogenised to powder and analysed using a CE-440 elemental analyser (Exeter Analytical). Combustion was at 975 °C, with detection by thermal conductivity.

3.4. Siliceous microfossils

Subsamples of 0.07–0.21 g wet sediment were prepared following Renberg (1990) with absolute diatom abundances determined following Battarbee & Kneen, (1982). Slides were mounted in Naphrax® and random fields were scanned at 1000× magnification on an Olympus CX 41 microscope. At least 400 valves were counted in each sample which was enough to capture the taxonomic richness of the assemblage. Marine diatom taxonomy followed Roberts and McMinn (1999) and Cremer et al. (2003) and freshwater diatoms followed Patrick and Reimer (1966), Round et al. (1990), Van de Vijver and Beyens (1997), Van de Vijver et al. (2002), Sabbe et al. (2003), Cremer et al. (2004), Van de Vijver et al. (2010) and Sterken et al. (submitted for publication).

The diatom stratigraphy was divided into zones using stratigraphically constrained cluster analysis (CONISS; Grimm, 1987) and plotted using Tilia 2.0.b.4 (Grimm, 1991–1993) and Tilia Graph View version 2.0.2. (Grimm, 2004). The significance of the zones was assessed using the broken stick model (Bennett, 1996) in the rioja package for R (Juggins, 2009). Changes in the diatom communities were interpreted following previously published ecological preferences of indicator taxa, in addition to quantitative relationships established between lacustrine diatom communities and environmental variables on Livingston Island (45 lakes, South Shetland Islands; 62°40′S, 61°00′W) Signy Island (24 lakes, South Orkney Islands; 60°43′S, 45°38′W; Jones et al., 1993), and Beak Island (6 lakes; Sterken et al. unpubl. data).

The siliceous cysts of chrysophytes and scales/plates of testate amoebae were also counted. Scales were identified following Douglas and Smol (2001), and mostly assigned to the genus *Euglypha*. It is possible that a few (less than 10%) belonged to the genus *Assulina* (see Douglas and Smol, 2001 for a review).

3.5. Fossil pigments

Fossil pigments were extracted from bulk sediments following standard protocols (Wright et al., 1991). All samples were freeze dried followed by immediate pigment extraction by sonication (30 s at 40 W) in 2–5 ml high-performance liquid chromatography (HPLC)-grade acetone (90%), and filtration of the extracts through a nylon filter (mesh size 0.20 um) to remove fine particles.

Pigments were separated and quantified using an Agilent technologies 1100 series HPLC with an autosampler cooled to −10 °C, a diode array spectrophotometer (400–700 nm), absorbance and fluorescence detectors. A reversed phase Spherisorb ODS2 column was used (internal diameter: 4.6 mm, particle size of 5 pm) with a gradient of three solvents (Wright et al., 1991; Method A). The HPLC system was calibrated using authentic pigment standards and compounds isolated from reference cultures following Scientific Committee on Oceanic Research (SCOR) protocols (Jeffrey et al., 1997). The taxonomic affinities of the pigments were derived from Jeffrey et al. (1997) and Leavitt and Hodgson (2001). To calibrate pigment derivatives the response factor of the native pigment was used, and for unidentified carotenoids a mean carotenoid response factor was applied.

4. Results

4.1. Limnology

The lake was circumneutral with pH ranging from 7.37 at the surface to 6.87 at the bottom (Table 1). Water temperature on the day of sampling was 4.82 °C (surface) and 4.26 °C (bottom). Salinity was 0.13–0.14 PSU, and conductivity and specific conductivity ranged between 172 and 177 μS/cm and 280–293 μS/cm respectively. Nutrient levels and ion composition were relatively low and below detection limits for both ammonium and nitrite, which is similar to other lakes and ponds on the island (Table 1).

4.2. Geochronology

The 1.66 m master core consisted of two drives (BK-1E and BK-1D). Twenty two samples from this core were ^{14}C dated (Table 2). The sediments are Holocene in age with a median basal calibrated age of 10,612 cal yr BP, and modelled age of 10,602 cal yr BP. The surface had a 'modern' percentage modern carbon (pMC) value, suggesting no freshwater radiocarbon reservoir effects prior to 1950. In general, radiocarbon ages were in stratigraphic order with exceptions at 15.5 cm and 32.5 cm, and at 103.5 and 129.5 cm depth. The exceptions at 15.5 cm and 32.5 cm may have been the result of translocation of some surface moss fragments from the dense, 5 cm thick moss layer, which required a considerable effort to penetrate during coring, although all macrofossil samples for dating were taken from the central part of the cores. Alternatively, these radiocarbon ages from aquatic mosses, which are adjacent to prominent volcanic ash (tephra) layers T_a and T_b (Fig. 3) may be compromised, either by reworking following catchment disturbance and/or due to possible changes in local-regional atmospheric ^{14}C equilibrium associated with large volcanic eruptions, as found in our recent studies on the South Shetland Islands (Watcham et al., 2011). As the influence of the latter is relatively poorly understood in this region, we have excluded these two radiocarbon age outliers. The exceptions at 103.5 and 129.5 cm, where ages of 10,901 ± 53 and 10,752 ± 62 ^{14}C BP were older than the basal sediment age of 10,625 ± 54 ^{14}C BP (166–167 cm depth; Fig. 3) possibly reflect the incorporation of older sediments, or marine derived material with a reservoir effect. The presence of distinct sedimentological lithofacies (Fig. 3), and clear stratigraphic zones in diatom and pigment compositions (Figs. 4 and 5) between 167 and 100 cm do not suggest major reworking of this sediment unit, which, with a sill height at c. 7–8 m below sea level at the time of deposition (Hodgson et al. unpubl. data), was protected from large-scale disturbances by marine currents or icebergs. Therefore, our age model rejects these dates and treats the dates below 108 cm as minimum ages.

Table 1
Summary of limnological measurements in Beak Lake 1 compared with limnological measurements from Beak Lakes 2–6, also on Beak Island (Fig. 2b). Surface and vertical profiles of lake water conductivity, temperature and oxygen saturation were measured using a YSI MDS 600 water quality meter. Water samples were collected in acid-washed Nalgene bottles. Analyses followed the procedures described in Hodgson et al. (2009b).

Sample	Temp (°C)	Sp. cond. (μS/cm^2)	Cond. (μS/cm)	Salinity PSU	DO_2 (%)	DO_2 (mg/l)	pH	Altitude sill (m)	Max. dept h (m)
Beak 1 surface	4.8	280	172	0.13	107.5	13.79	7.4	10.95	24
Beak 1 bottom (24 m)	4.3	293	177	0.14	80.3	10.38	6.9		
Beak 2	12.2	250	188	0.12	112.5	12.05	8.6	2.365	4
Beak 3	14.3	311	247	0.15	111.3	11.46	8.9	0.515	1
Beak 4	12.8	612	470	0.3	114.1	12.03	9.8	–	0.5
Beak 5	12.8	312	239	0.15	115.3	12.2	9.1	–	0.5
Beak 6	13.3	272	212	0.13	110.2	11.57	9.2		0.5

Sample	NO_3–N (mg/l)	NH_4–N (mg/l)	PO_4–P (mg/l)	Si (mg/l)	Cl^- (mg/l)	TDN (mg/l)	Na (mg/l)	K (mg/l)	Mg (mg/l)	Ca (mg/l)
Beak 1	<0.1	<0.01	0.017	1.22	68.8	0.14	37.7	2.0	6.57	5.05
Beak 2	<0.1	0.025	0.006	0.35	59.6	0.49	34.2	2.5	5.97	3.7
Beak 3	<0.1	0.021	<0.005	0.89	73.6	0.58	40.9	3.1	8.67	5.24
Beak 4	<0.1	<0.01	<0.005	2.97	144	1.7	108	6.5	8.55	3.72
Beak 5	<0.1	0.045	0.041	0.70	68.7	0.57	39.4	3.4	10	4.87
Beak 6	<0.1	<0.01	<0.005	1.07	62.5	0.66	31.1	4.1	8.96	4.86

Sample	TOC (mg/l)	DOC (mg/l)	SO_4–S (mg/l)	Al (mg/l)	Fe (mg/l)
Beak 1	0.75	0.99	3.27	0.126	0.109
Beak 2	2.4	2.67	3.32	0.009	0.018
Beak 3	3.1	3.86	4.66	0.011	0.045
Beak 4	7.7	11	10	0.079	0.063
Beak 5	2.9	3.25	6.01	0.035	0.084
Beak 6	4.3	4.62	3.51	<0.002	0.093

Geochemical analysis of glass shards in tephra deposits in the core permitted comparisons with the regional tephrochronology and provided independent constraints on the radiocarbon ages. Five black (basic-intermediate) visible volcanic ash (tephra) horizons in the Beak Lake 1 core were characterized by higher MS values and lower organic content compared to their bracketing sediments. These include a prominent c. 2 cm thick black tephra 'layer' at 32–34 cm (Fig. 4; T_b), a 1 cm thick layer at c. 58–59 cm (T_d), and an 8–10 cm thick airfall and reworked tephra deposit between 130 and 140 cm depth (T_e), and a number of other minor tephra. We provisionally linked these tephra deposits to previously published ages for tephras from the Deception Island volcano (180 km to the west) as follows: T_a (16–17 cm, 1981–2028 cal yr BP) may be equivalent to the relatively small eruption between 900 and 1500 cal yr BP (Björck et al., 1991c, 1993; Hodgson et al., 1998) or 800–1000 cal yr BP (Watcham et al. (2011), or may comprise reworked material from T_b; T_b (32–34 cm, 2260–2329 cal yr BP) may be equivalent to the 2300–2800 cal yr BP eruption (Bjorck et al., 1991c) or 2200–2400 cal yr BP (Watcham et al., 2011); T_c (44.45 cm, 3169–3286) may be equivalent to the 3310 ± 70 yr BP eruption (dated using relative palaeomagnetic intensity data, Willmott et al., 2006); T_d (58–60 cm, 4788–5043 cal yr BP) may be equivalent to the 5000 ± 70 yr BP eruption (Willmott et al., 2006) or c. 4800–5000 cal yr BP (Watcham et al., 2011); T_e (c. 130–140 cm, 9868-10081) is possibly the result of an unreported eruption from Deception Island between c. 10,000–11,000 yr BP. It has a geochemical shard geochemistry more commonly associated with eruptions from Deception Island rather than, for example, the 10700 yr BP eruption from the South Sandwich Islands found in the EPICA Dome C ice core (Smellie, 1999, 2001; Fretzdorff and Smellie, 2002; Risso et al., 2002; Narcisi et al., 2005), the only other major eruption with geochemical data from this area in the 11000–7000 yr BP interval. We acknowledge that it could also be related to the explosive eruption at c. 7000–7500 yr BP (Lee et al., 2007; Watcham et al., 2011), which is probably equivalent to the 6920 yr BP eruption based on relative palaeomagnetic intensity data reported in Willmott et al. (2006). This alternative scenario is indicated by a dashed line with question marks in Fig. 3, but is considered unlikely based on preliminary ice core data from James Ross Island (R. Mulvaney, pers. comm.). Further work on the major element geochemistry of these deposits will help refine this regional tephrochronology,

4.3. Sedimentological properties

Seven distinct lithological units were observed with well defined transitions (Fig. 3). The base of the core was composed of coarse gravel that prevented deeper penetration of the corer, overlain by gravelly sand, gravel, sand and mud (166–147 cm). From 147–102 cm, lenses of gravel, sand, fine sand and silt were embedded in a black organic mud matrix, and overlain by a unit of dark grey/black fine organic mud (102–75 cm). The main lithological change in the core occurred at c. 75 cm, where greenish-grey fine organic muds were overlain by a unit of light greenish-grey to olive green clay rich laminated sediments composed of decayed cyanobacterial mats (74–45 cm) and a unit of olive green, fine organic mats (45–30 cm). A unit of olive green laminated fine organic mud/mats occurred between c. 28–5 cm and there were abundant moss macrofossils in the uppermost 5 cm of the core. Moss macrofossils were also present at 17.5–15 cm and 33–32 cm and in small quantities between 20 and 9 cm. There was no evidence of slumps or other discontinuities in the core and the upper c. 70 cm was finely laminated.

Visible tephra layers T_{a-e} corresponded to peaks in magnetic susceptibility (MS) and troughs in LOI (Fig. 4). With the exception of the tephra layers, MS was generally highest where coarse gravels to silts were present (Fig. 4). Wet density also tracked the presence of the coarser sediment fractions, declining markedly in the organic units above 75 cm (Fig. 4). LOI_{925}, a proxy for carbonate content, was fairly constant between c. 5–9% throughout the core, with the exception of minima in the tephra layers and a sharp drop to c. 4% above 20 cm depth (Fig. 4). LOI_{550}, a proxy for organic content, remained below 3.5% between 166 and 105 cm associated with the coarser sediment fractions, and only rose above 5% after the transition into more organic cyanobacterial mat/organic-rich mud remains above 96 cm depth. A peak in LOI_{550} occurred at the main transition at 75 cm. A long and sustained peak occurred between 45 and 25 cm, with its maximum at 30 cm briefly interrupted by tephra layer (T_b) at 33 cm . Organic content (LOI_{550}) increased from 10 cm towards the top of the core, with the minor decrease in the top 2 cm being an artefact of the removal of the moss macrofossils from the analytical samples. The C/N ratio was lowest below 75 cm and increased towards 15.9 at 72.5 cm (Fig. 4) maintaining relatively high values until 27.5 cm. Low C/N values were present between

Table 2
Radiocarbon dates for the Beak Lake 1 sediment core. Calibration of ^{14}C age data is as follows: calibration models: A = CALIBomb SH1, a compilation of Southern Hemisphere datasets ((Hua and Barbetti, 2004); http://calib.qub.ac.uk/CALIBomb/), using the absolute percentage of modern carbon (pMC) data, corrected according to $^{13}C/^{12}C$ isotopic ratios from measured pMC, where 'modern' is 1950 AD and 100 pMC, and 'present day' is defined as 2010 and 107.5 pMC; B = SHCal04.^{14}C atmosphere (McCormac et al., 2004); http://calib.qub.ac.uk/calib/calib.html) where cal yr BP = yr before 1950 AD; C = 50% SHCal04.^{14}C atmosphere, 50% MARINE09 mixed model; D = Intcal09.^{14}CMarine with ΔR set to 880 ± 50 to account for the local marine reservoir offset see text (Reimer et al., 2009).

Lab/Publication code	Core ID & depth	Stratigraphic depth (cm)	Summary description	Carbon source	Marine/ Lacustrine	Carbon content	$\delta^{13}C_{VPDB}$	pMC/^{14}C enrichment	Conventional radiocarbon age	2σ calibrated age data (A = yr AD; B-D = cal yr BP)			
						(wt %)	(‰)	(% modern ± 1σ)	(years BP ± 1σ)	Min. − Max	Rel. Prob.	Median prob.	Age Model
BEAK LAKE 1													
SUERC-12385	BK1E: 0–1	0–1	Fine strands aquatic moss *Cratoneuropsis chilensis*	Macrofossil	Lacustrine	44.2	−32.4	108.6 ± 0.5 107.9 ± 0.5[a]	modern	>2004 AD or 1957–1958	1.00 0.00	>2004 AD 1958 AD	A A x
BETA-288864	BK1E: 2.5	2.5–3	Fine strands aquatic moss *C. chilensis*	Macrofossil	Lacustrine	26.8	−26.5	122.2 ± 0.5 122.5 ± 0.5[a]	modern	1982–1986 1961–1962	0.86 0.11	1984 AD 1961 AD	A
BETA-288865	BK1E: 4	4–4.5	Fine strands aquatic moss *C. chilensis*	Macrofossil	Lacustrine	43.0	−27.1[a]	94.1 ± 0.5	490 ± 40	451–545	0.98	505	B
BETA-288866	BK1E: 8.5	8–8.5	Fine strands aquatic moss *C. chilensis*	Macrofossil	Lacustrine	4.2	−25.4	81.4 ± 0.5	1650 ± 50	1368–1607	1.00	1477	B
BETA-288867	BK1E: 12	12–12.5	Olive green fine organic mud/mat	Mat (TOC)	Lacustrine	2.8	−28.4[a]	79.8 ± 0.4	1810 ± 40	1557–1742 1753–1811	0.90 0.10	1663	B
SUERC-12394	BK1E: 15.5	15.5–16	Greenish-grey laminated fine organic mud	Mat (TOC)	Lacustrine	1.4	−26	82.3 ± 0.4	1563 ± 35	1311–1424 1457–1516	0.78 0.19	1390	B[b]
Not analysed	BK1E: 15.5	15.5–16	Very fine strands aquatic moss *C. chilensis*	Macrofossil	Lacustrine	*Insufficient material for AMS dating; 2 attempts*							- x
SUERC-12395	BK1E: 31	31–32	Olive green fine mud/light grey clay laminations	Mat (TOC)	Lacustrine	9.3	−29.8	75.1 ± 0.3	2305 ± 35	2153–2277 2289–2344	0.69 0.32	2235	B
SUERC-12386	BK1E: 32–33	32–33	Fine strands aquatic moss *C. chilensis*	Macrofossil	Lacustrine	30.0	−28.9	87.2 ± 0.4	1101 ± 35	914–1015 1023–1055	0.87 0.13	957	B[b]
SUERC-12396	BK1E: 34	34–35	Consolidated medium-dark olive green mud/mat	Mat (TOC)	Lacustrine	11.4	−31.4	74.7 ± 0.3	2345 ± 35	2297–2355 2157–2265	0.54 0.46	2307	B
SUERC-12397	BK1E: 43.5	43–44	Light grey-olive green fine organic mud/mat	Mat (TOC)	Lacustrine	6.7	−30.4	69.4 ± 0.3	2940 ± 35	2918–3160	0.95	3018	B
SUERC-12398	BK1E: 46	46–47	Light grey-olive green fine organic mud/mat	Mat (TOC)	Lacustrine	4.0	−29.3	66.5 ± 0.3	3280 ± 35	3370–3511 3518–3557	0.89 0.11	3441	B
SUERC-12401	BK1E: 55	55–56	Light grey-olive green fine organic mud/mat	Mat (TOC)	Lacustrine	4.1	−29.9	60.4 ± 0.3	4048 ± 35	4384–4571	0.96	4473	B
SUERC-12402	BK1E: 59	59–60	Light grey-olive green fine organic mud/mat	Mat (TOC)	Lacustrine	3.0	−30.2	58.2 ± 0.3	4346 ± 35	4816–4972	0.97	4857	B
SUERC-12403	BK1E: 73.5	73–74	Medium-light olive green fine organic mud/mat	Mat (TOC)	Transition end	9.6	−26.7	47.3 ± 0.2	6010 ± 36	6674–6888	1.00	6783	B
SUERC-12564	BK1D: 8.5	73–74	Medium-light olive green fine organic mud/mat	Mat (TOC)	Transition end	8.7	−27.8	46.8 ± 0.2	6098 ± 35	6781–7001	0.99	6890	B
SUERC-12404	BK1E: 78.5	78–79	Dark greenish-grey/black fine organic mud	Bulk (TOC)	Transition start	3.1	−22.4	43.2 ± 0.2	6735 ± 35	6797–7088	0.97	6944	C
SUERC-12565	BK1D: 14.5	79–80	Dark greenish-grey laminated organic mud	Bulk (TOC)	Transition start	1.2	−22.5	39.8 ± 0.2	7393 ± 36	7508–7672	1.00	7596	C
SUERC-12943	BK1D: 38.5	103–104	Dark greenish-grey laminated fine organic mud	Bulk (TOC)	Marine	0.3	−21.9	25.7 ± 0.2	10901 ± 53	10734–11173	1.00	10993	D x
SUERC-12566	BK1D: 43.5	108–109	Laminated organic mud with coarse sand/silt and clay	Bulk (TOC)	Marine	0.2	−21.5	30.2 ± 0.2	9626 ± 48	9255–9532	1.00	9418	D
SUERC-12944	BK1D: 64.5	129–130	Clay rich black volcanic silty sand (reworked?)	Bulk (TOC)	Marine	0.2	−20.6	26.2 ± 0.2	10752 ± 62	10578–11069	1.00	10796	D[b]
SUERC-12945	BK1D: 75.5	140–141	Clay rich black volcanic silty sand (airfall?)	Bulk (TOC)	Marine	0.2	−21.2	28.3 ± 0.2	10147 ± 46	9873–10238	1.00	10090	D
SUERC-12567	BK1D: 101	166–167	Dark greenish-grey/black coarse sand and silt/clay bands	Bulk (TOC)	Marine	0.3	−21.5	26.6 ± 0.2	10625 ± 54	10461–10892	1.00	10612	D

'x' = age omitted from age-depth model due to ages being out of sequence or reworking of older sediment.
[a] Indicates absolute pMC. Probabilities with a total sum >0.95 are shown.
[b] Ages adjacent to visible volcanic ash layers were omitted from the age model (see Methods).

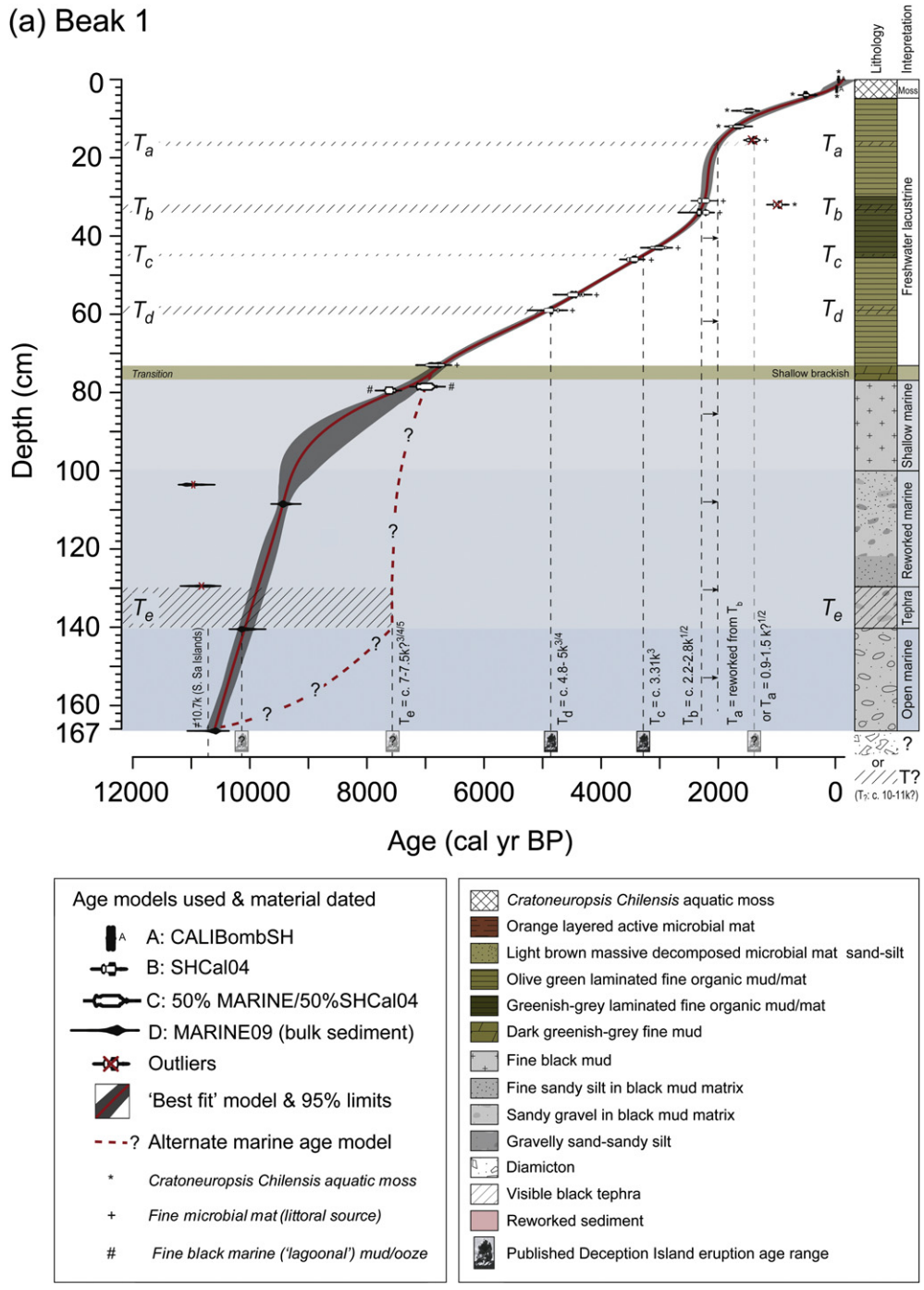

Fig. 3. Stratigraphic age-depth plot undertaken in CLAM (Blaauw, 2010) and lithology of the Beak Lake 1 sediment core. CLAM settings: smooth spline (smoothing 0.3); 1000 iterations weighted by calibrated probabilities at 95% confidence ranges and resolution 1 year steps. CLAM output statistics: 0–166 cm; 350 models with age reversals were removed; – log goodness of fit = 139.09; 95% confidence range 126–1006 years, mean 306 years. Tephra references: 1 = Björck, et al. (1991c); 2 = Hodgson et al. (1998); 3 = Wilmott et al. (2006); 4 = Lee et al. (2007); 5 = Watcham et al. (2011).

20.5 and 9.5 cm, and slightly higher values occurred in the top 9 cm of the core, including peaks at 8.5 and 3.5 cm (Fig. 4).

4.4. Siliceous microfossils

The diatom stratigraphy of the Beak-1 core was divided into 6 zones based on a CONISS cluster analysis of the diatom species composition (Fig. 4). A broken stick analysis showed that three of these zones were significant (Zones 1 + 2, Zone 3, Zones 4 + 5). The non-significant ones were retained because they correspond to marked changes in other siliceous microfossil groups and in sedimentological properties in the core (Fig. 4).

Diatom Zone 1 (166–105 cm) was characterized by very low total diatom concentrations including 23–45% broken valves and a moderate species richness of 15–25 species (Fig. 4). The diatom communities comprised a mixture of marine and sea ice related taxa, such as *Navicula glaciei* (12–31%), *Achnanthes brevipes* (15–31%) and *Navicula perminuta* (6–10%), and open water marine

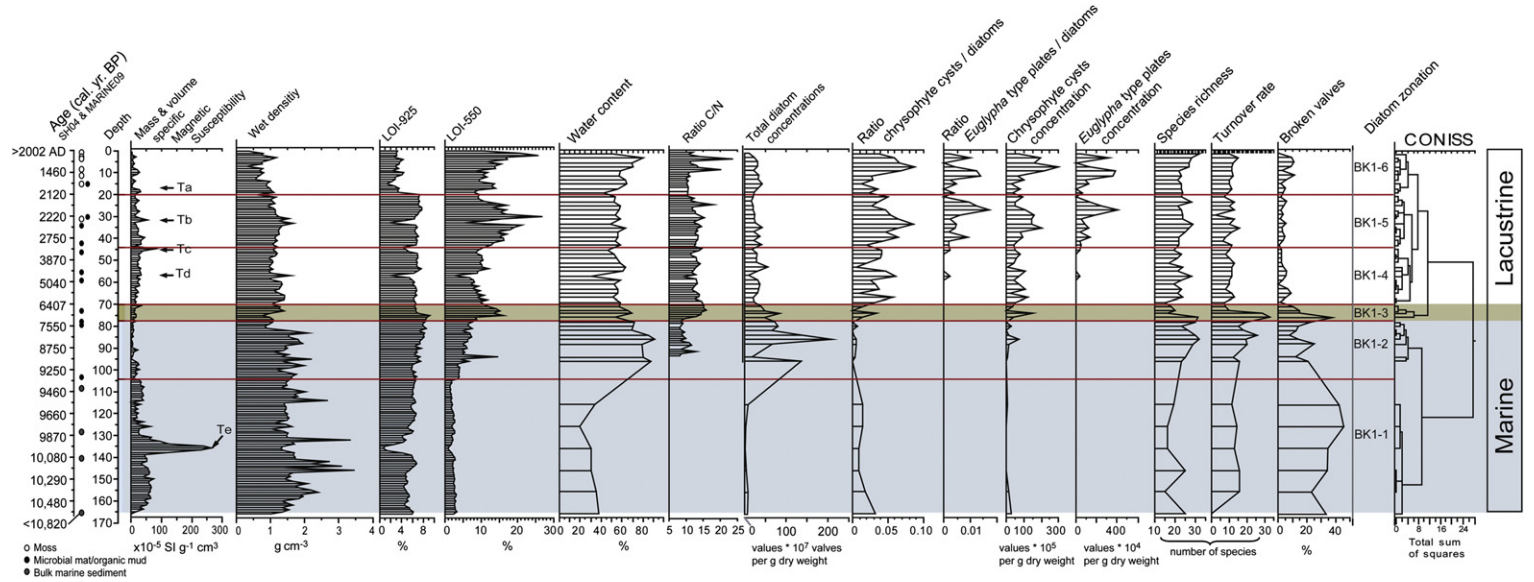

Fig. 4. Sedimentological, geochemical and microfossil-based proxies in the Beak-1 sediment core, plotted against depth (cm). Corresponding interpolated calibrated ages are given, and depths of ^{14}C dates (Table 2 and Fig. 3) are indicated by black dots. LOI stands for organic content measured by % weight loss on ignition (LOI_{550}; after combustion at 550 °C for 2 h) and carbonate composition (LOI_{950}; % weight loss after combustion at 950 °C for 2 h). The ratio of stomatocysts to diatoms and the total abundance of cysts are used as measures of the amount of planktonic chrysophytes. Diatom species richness is the number of taxa in each sediment sample. The diatom turnover rate is calculated as the sum of the number of taxa gained and the number of taxa lost when moving from one sample to the next (in order of deposition). The number of broken diatom valves is calculated as a percentage of the total number of diatoms counted, with the exclusion of *Chaetoceros* RS. The zonation of the core is based on the CONISS analysis of the diatom species compositions (Fig. 5). Ta, Tb, Tc and Td represent the tephra layers in the core.

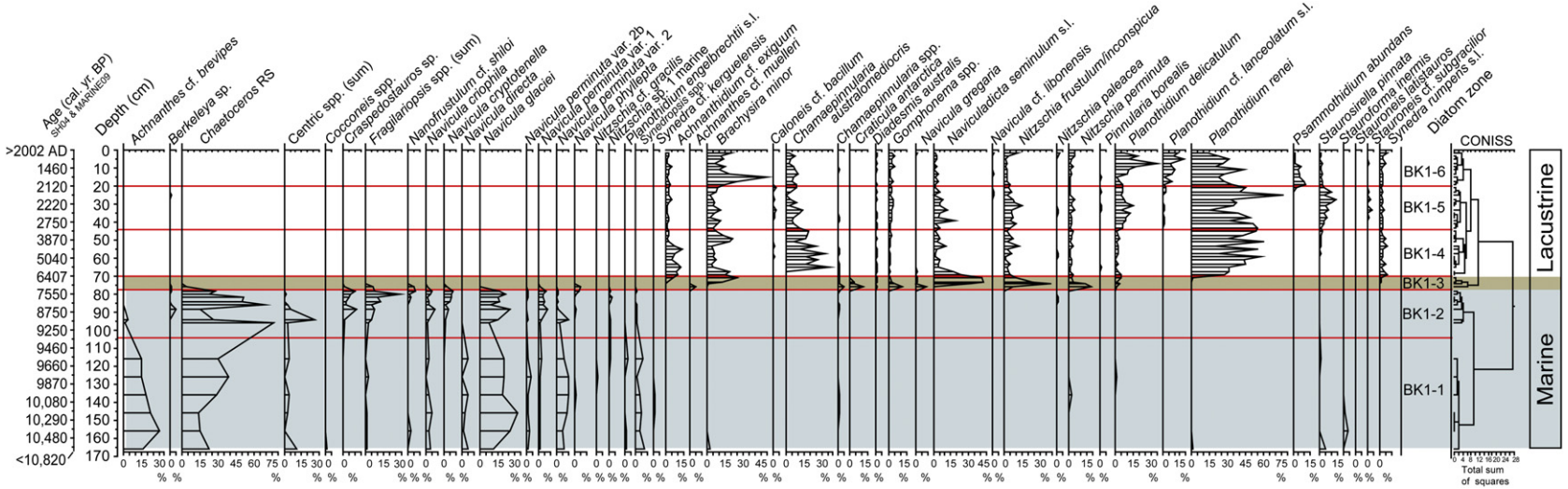

Fig. 5. Diatom stratigraphy of the Beak-1 sediment core, plotted against depth (cm) and age. Ages are calibrated and corrected for marine reservoir effects. Corresponding interpolated calibrated ages are given, and depths of ^{14}C dates (Table 2 and Fig. 3) are indicated by black dots. Only diatom species with a relative abundance exceeding 5% or occurring in five or more samples are shown, as well as selected species with a specific (ecologically meaningful) distribution in the core. *Chamaepinnularia* spp. includes a combination of *C. gerlachei*, C. sp. 2, *C.* sp. 3 and *C. cymatopleura*. Centric species are summed, as well as all species of the genera *Cocconeis* and *Fragilariopsis*. Photomicrographs of key diatom species are presented in Sterken et al. (submitted for publication). Zonation of the core is based on a CONISS analysis of the diatom species compositions.

taxa such as *Chaetoceros* resting spores (CRS) (13–29%) (Fig. 5). Occasional freshwater diatoms valves were present, with *Staurosirella pinnata* reaching a maximum of 5% in the basal sample.

In Diatom Zone 2 (105–76 cm) total diatom concentrations increased to their highest abundance of 210×10^7, the fraction of broken valves decreased to 7–37%, and species richness increased slightly to 23–32. Total diatom concentrations were very variable, largely as a result of changes in CRS, reaching relative abundances of up to 76.7%. When CRS abundances dropped at 94 and 88 cm depth, *Navicula glaciei* became co-dominant (up to 25%) together with centric species (25% at 94 cm) and *Craspedostauros* and *Berkeleya* species (11% and 5% at 88 cm, respectively) (Fig. 5). Other (spring) sea ice related species (e.g., *Fragilariopsis* spp.; Armand et al., 2005; Crosta et al., 2008), and brackish-water diatoms (e.g., *Craspedostauros* sp.) became increasingly abundant in this zone with *Fragilariopsis* spp. reaching 28%, whilst *Achnanthes* cf. *brevipes* declined.

Diatom Zone 3 (76–70 cm) included a clear transition from marine to freshwater diatom assemblages coinciding with the marked transition in lithology at 75 cm depth (Figs. 3 and 5). Diatom species richness (15–31), turnover rate (8–33) and percentage of broken valves (10–38%), all reached their maxima between 76 and 74 cm depth, and all reached their minima between 73 and 71 cm, immediately after the transition. Diatoms were dominated by taxa characteristic of lakes with relatively high production (e.g., *Nitzschia perminuta* (2–19%), and *Nitzschia frustulum* (7–39%), *Gomphonema* spp. (2–11%)), and taxa known to have a broad salinity tolerance, for example *Craticula antarctica* (4–11%) between 76 and 74 cm, and by *Naviculadicta seminulum* (45%) and *Brachysira minor* (12–25%) between 73 and 70 cm depth (Fig. 5).

In Diatom Zone 4 (70–44 cm) *Planothidium renei* was the dominant taxon and its abundance varied widely from 19 to 60% (Fig. 5). *Achnanthidium* cf. *exiguum*, *Chamaepinnularia australomediocris* and *P. renei* appeared at 70–67 cm depth and maintained relative abundances of 2–13%, 15–76% and 19–55% respectively. *A.* cf. *exiguum* declined sharply from 13% to 2% above 49 cm and *C. australomediocris* gradually declined towards the top of the core. The number of broken valves fell to <10%, and species richness was a fairly constant 21–27 from here to the top of the core. *Euglypha* type plates appeared for the first time in this zone (Fig. 4).

Diatom Zone 5 (44–20 cm) was marked by an increase in the concentration of stomatocysts and *Euglypha* type plates to $77–277 \times 10^5$/g and $82–416 \times 10^4$/g respectively. The former can be an indicator of low productivity in temperate lakes, but have been correlated with the presence of mosses and/or with lake ice cover in high latitude lakes (Smol, 1983, 1988; Douglas and Smol, 1995; Zeeb and Smol, 2001). The latter are often associated with moss habitats in sub-Antarctica (Vincke et al., 2006), and acid peats and bogs (Smith, 1992). The diatoms in this zone were again dominated by *P. renei* (15–76%), with a minor increase in *Planothidium delicatulum* (5–15%), by the appearance of the tychoplanktonic diatom *S. pinnata* rising to a maximum abundance of 13% at 27 cm depth, and the presence of aerophilic taxa such as *Stauroneis* cf. *subgracilior*, *Caloneis bacillum*, *Mayamaea atomus* var. *permitis* and *Diadesmis* spp. (Fig. 5), at relative abundances below 5%.

In Diatom Zone 6 (20–0 cm) *P. renei* remained dominant (13–44%), but was replaced briefly by the dominance of the moss-associated *B. minor* reaching 50% at 14 cm (Fig. 5). *B. minor* started its increase from 20 cm which coincided with the appearance of *Psammothidium abundans*, a diatom common in deep freshwater (>5 m) lakes in the Larsemann Hills (Verleyen et al., 2003), and indicative of low phosphorous concentrations and high light intensities. The appearance of this latter species also coincided with a marked decline in carbonate content (LOI_{950}) at 20 cm depth (Fig. 4). *P. delicatulum* increases up to 35%. This species currently occurs in low-elevation lakes in Signy and Livingston islands, is epilithic, found at sea spray associated sites and/or in meltwater streams (Jones et al., 1993; Jones & Juggins, 1995; Sterken et al. unpubl. data). *Planothidium lanceolatum* increased through this zone towards the top of the core. This species is currently found in high-elevation, low productivity lakes with low nutrient concentrations (Jones et al., 1993; Jones and Juggins, 1995; Sterken et al. unpubl. data). *Euglypha* type plates and stomatocysts were also abundant in this zone increasing to zone maxima of 387×10^4/g and 271×10^5/g respectively (Fig. 4), before declining towards the top of the core. In the uppermost core sediments there was a moderate increase in species richness to 30 from a zone mean of 23.5 and an increase in the abundances of *N. frustulum* from <3% to 11.7%. This species was also abundant in Zone 5, and immediately after the transition in Zone 3.

4.5. Fossil pigments

Changes in total pigment concentrations and relative abundances in the core were broadly consistent with the lithological and diatom zones (Fig. 6). Independent cluster analysis of the pigment relative abundance data shows that there are two lower zones, a transitional zone, and two upper zones (Fig. 6).

In Pigment Zone I (165–145 cm) total pigment concentrations were low with a mean of 20 μg/g of caroteoids and 26 μg/g of chlorophylls. The carotenoids included pigments produced by marine diatoms, dinophytes and chrysophytes (diatoxanthin), and chlorophytes (lutein). β,β-carotene (chlorophytes and cyanobacteria) and chlorophyll derivatives, including (pyro)phaeophitin *a* were relatively abundant. Occasional occurrences of terrestrial/lacustrine cyanobacteria specific pigments (myxoxanthophyl, canthaxanthin) suggest the presence of material of both marine and terrestrial origin.

Pigment Zone II (145–86 cm) was defined by a marked increase in carotenoid concentrations to a mean of 104 μg/g and a moderate increase in chlorophylls to 67 μg/g, suggesting and increase in phototrophic production or pigment preservation. Pigment composition remained similar, being dominated by a derivative of β,β-carotene, and fucoxanthin, which is present in diatoms and chrysophytes, became more abundant above 105 cm. Of the chlorophyll derivatives pyrophaeophytin *a* was near absent in the lower part of the zone, being replaced by native chlorophyll *a* and chlorophyll *a* derivative 2. Total carotenoid and chlorophyll concentrations increased towards the top of the zone but this increase was not seen as an increase in the total organic content (LOI_{550}, Fig. 4).

Pigment Zone III (86–70 cm) spanned the Diatom Zone 3 transition between marine and freshwater diatoms, but starts slightly earlier at 86 cm. Total concentrations of chlorpohylls and carotenoids were highly variable ranging from 34 to 302 μg/g and 17–379 μg/g, respectively. There was an increase in the number of pigment derivatives with some, such as Phaeophorbide *a* and Phaeophytin *b* appearing for the first time, and others such as chlorophyll *a* derivative 2, and a derivative of β,β-carotene becoming near absent. Zeaxanthin appeared for the first time above 70 cm depth, lutein and phaeophytin *b* (indicative of chlorophytes and bryophytes; Leavitt and Findlay, 1994) reached their maxima in this zone, and at 74 cm depth, small peaks similar to hexanoyloxifucoxanthin, canthaxanthin and vaucheriaxanthin were also present.

Above the transition in Pigment Zone IV (70–44 cm) there was a marked decline in pigment concentrations with means of 2.3 and 80 μg/g for carotenoids and chlorophylls respectively. Many

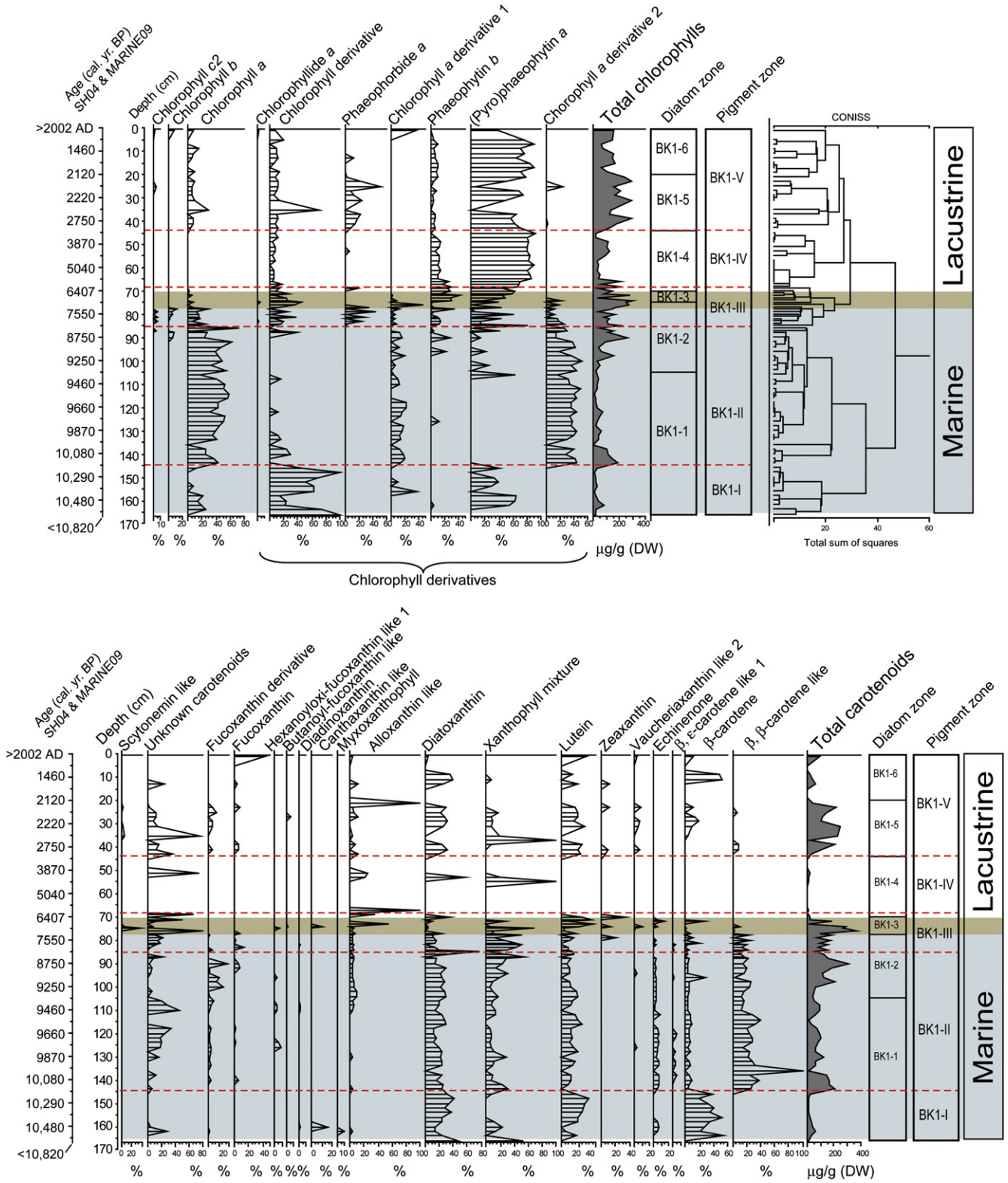

Fig. 6. Fossil pigment stratigraphy of the Beak-1 sediment core, plotted against depth (cm). Corresponding interpolated calibrated ages are given, and depths of ^{14}C dates (Table 2 and Fig. 3) are indicated by black dots. Only pigments constituting more than 2% of the total carotenoids or total chlorophylls are shown. Total pigment concentrations (grey shaded graphs) are expressed in µg/g dry weight (DW). Zonation of the core is based on a CONISS analysis of the pigment composition.

carotenoids were below detection limits whilst pyrophaeophytin *a* dominated the chlorophylls and phaeophytin *b* was subdominant.

In the upper Pigment Zone V (44-0) there was a clear peak in total chlorophyll and total carotenoid concentrations between 44 and 20 cm (129 and 200 µg/g respectively, which corresponds exactly with Diatom Zone 5, and a marked peak in the organic content. There was also an increase in pigment diversity with pigments produced in diatoms, cryptophytes and cyanobacteria and green

algae/mosses, including fucoxanthin and its derivatives, diadinoxanthin, diatoxanthin, lutein, vaucheriaxanthin-like pigments and β,β-carotene. Non-degraded chlorophyll *a* and phaeophorbide *a*, a pigment produced under grazing conditions reappeared in this zone together with a peak of alloxanthin-like pigments (almost 100% at 21 cm depth). Above 20 cm, pigment concentrations declined again with means of 24 μg/g and 118 μg/g for carotenoids and chlorophylls respectively. Some samples were devoid of carotenoids, and contained only small concentrations of chlorophyll-derived pigments, which coincided with the marked shifts in diatom communities (Fig. 5). The uppermost sample was distinguished only by minor peaks in fucoxanthin together, lutein, β,β-carotene, chlorophyll *b* (likely related to mosses) and a chlorophyll *a* derivative.

5. Discussion

5.1. 10,602–9372 cal yr BP: deglaciation and the establishment of perennial sea ice

The minimum modelled age of deglaciation of Beak Island is c. 10,602 cal yr BP based on the onset of marine sedimentation. Sedimentological analyses of a suite of cores from the outer to inner marine continental shelf provide the earliest constraints on deglaciation of Antarctic Peninsula Ice Sheet and the onset of post glacial marine deposition in the glacial troughs in this region. In southern Prince Gustav Channel (southwest of James Ross Island near the Larsen Ice Shelf, Fig. 1b,1) deglaciation commenced from an inferred maximum of c. 16,700 ^{14}C yr BP (19,950 cal yr BP) (Pudsey et al., 2006), but the reservoir effect was large (i.e., ≥6000 years) so dating-control is limited. To the east, ice retreat from the outermost continental shelf had commenced sometime after 20,319 cal yr BP in the NW Weddell Sea (Smith et al., 2010, Fig. 1b, 2) and shelf edge at 18,510 cal yr BP (Heroy and Anderson, 2007, Fig. 1b, 3). Subsequent deglaciation of this trough towards Beak Island is poorly constrained in the marine geological record, but terrestrial radiocarbon dates and cosmogenic isotope ages from the surrounding islands provide evidence of deglaciation along the margins of the main trough. The nearest site (33 km south) is the southwest of Vega Island (Fig. 1b, 4) where estimates based on sediment containing organic material ('probably algae') between two moraine ridges was dated at 10,235 ^{14}C yr BP (11,911 cal yr BP) (Zale and Karlén, 1989), which just predates the Beak Island deglaciation, and 30 km southwest at Cape Lachmann on James Ross Island where Ingólfsson et al. (1992, Fig. 1b, 5) suggested an initial deglaciation around 9525 ^{14}C yr BP (10,718 cal yr BP) from moss deposits in a cliff section at <20 m altitude.

Interestingly, these deglaciation ages are similar to the minimum uncorrected ages of 10600, 9760 and 9210 ^{14}C yr BP (10,605, 9569 and 8832 cal yr BP) measured on foraminifera in two marine sediment cores obtained on the inner shelf of the north-western Weddell Sea (Domack et al., 2005, Fig. 1b, 6) and with a geomagnetic intensity age of 10,700 ± 500 yr BP from the inner Larsen-A Ice Shelf region (Brachfeld et al., 2003, Fig. 1b, 7) supporting a broadly synchronous disintegration of the north eastern part of the Antarctic Peninsula Ice Sheet on the inner continental shelf (cf. Hodgson et al., 2006a; Heroy and Anderson, 2007) at this time. The grounding line features and the nature of streamlined bed forms formed in deformation till in this region of the north-western Weddell Sea margin suggest that this retreat was continuous in the major troughs (including Prince Gustav Channel, Robertson Trough, and the troughs of the, Larsen-A and Larsen Inlet), but was staggered and punctuated by still stands across the mid-shelf (e.g., Northern Larsen-A, south of Prince Gustav Channel) (Evans et al., 2005). Reconstructions of relative sea level change at Beak Island also support this early Holocene deglaciation as regional isostatic uplift was sufficiently advanced to be outpacing eustatic sea level rise at a rate of 3.91 mm yr^{-1} by c. 8000 cal yr BP (Roberts et al. 2011).

A series of younger deglaciation ages has also been recorded on the islands flanking Prince Gustav Channel. These include cosmogenic isotope ages for deglaciation of 8000 ± 800 yr BP at a higher altitude of 120 m a.s.l. at Cape Lachmann on James Ross Island (Johnson et al. 2011, Fig. 1b, 5) and dates from the emplacement of glaciomarine deposits over glacial till between 8460 ± 90 and 7920 ± 60 ^{14}C yr BP (8023–7512 cal yr BP) at The Naze on James Ross Island which have been attributed, not to deglaciation, but to a glacial readvance (Ingólfsson et al., 1992, p. 213, Fig. 1b, 8). Further inland a short-lived readvance of glaciers into Brandy Bay between 5000 and 4500 ^{14}C yr BP (c. 5510–5080 cal yr BP) (Hjört et al., 1997, p. 271, Fig. 1b, 9) associated with the Bahía Bonita glacial drift (Rabassa, 1983; Björck et al., 1996) and proxy evidence of high water levels in Terrapin Lake (southern end of The Naze, James Ross Island, Fig. 1b,10) associated with 'probable' glacial advances between 4200 ^{14}C yr BP until around 3000 ^{14}C yr BP (4645–3110 cal yr BP) (Björck et al., 1996, p. 215).

Some of these younger chronological constraints are of similar ages to the deglaciation of other regional sites (not directly abutting PGC), for example cosmogenic isotope ages of 7500 ± 700 yr BP at Seymour Island (76 km to the southeast; Johnson et al. 2011, Fig. 1b, 11) and a minimum extrapolated age of deglaciation of ca 6300 ^{14}C yr BP (6735–7471 cal yr BP) (Zale, 1994b, p 183) obtained from a radiocarbon dating model applied to lake sediments for deglaciation of Hope Bay, 32 km north (Fig. 1b, 12).

Collectively these data suggest that the main deglaciation of Prince Gustav Channel took place around c. 10,602 cal yr BP and supports the hypothesis of Johnson et al. (2011) that, following Antarctic Peninsula Ice Sheet retreat onto the mid-shelf, grounded ice would have retreated from Prince Gustav Channel before the feeder glacier troughs and marginal terrestrial sites became ice-free. This minimum age for deglaciation is in phase with the early Holocene warm period between 11000 and 9500 yr BP detected in ice cores from the central plateau (Masson-Delmotte et al., 2004, 2011; Fig. 7) and lacustrine and shallow marine sediment cores from elsewhere in Antarctica (see Verleyen et al., 2011 for a review). It is however unlikely that warmer climate conditions alone led to the destabilisation of the Antarctic Peninsula Ice Sheet. Changing configurations of ocean currents, bringing warmer water onto the continental shelf and into contact with the grounded ice sheet, ice streams and floating ice (shelves) in combination with the rising global sea levels due to melting of the Northern Hemisphere ice masses at the start of the Holocene are also likely to have affected the stability of the marine based Antarctic Peninsula Ice Sheet. One theory is that the resulting meltwater from the Antarctic Peninsula Ice Sheet stratified the water column around the AP forming a meltwater lid and promoting the formation of sea ice. This could explain the lower diatom abundance and assemblages characteristic of more persistent sea ice recorded at Beak Island between 10602 and 9372 cal yr BP and in the Palmer Deep, on the north-western side of the AP between c. 12800 and 9000 yr BP (Sjunneskog and Taylor, 2002). Alternatively the increased sea ice at the Palmer Deep could indicate a regional climate reversal between 11000 and 9000 yr BP (Taylor and Sjunneskog, 2002), but would be inconsistent with ice core data (Masson-Delmotte et al., 2004, Fig. 7) and marine and lacustrine sediment cores from elsewhere in Antarctica (e.g., Verleyen et al., 2011).

Between c. 10,602–9372 cal yr BP (Diatom Zone 1, 166–105 cm) the sediments were interpreted as glaciomarine deposits derived from the decaying Antarctic Peninsula Ice Sheet, including iceberg rafted debris (e.g., Pushkar et al., 1999; Brachfeld et al., 2003; Domack et al., 2005). This was supported by the low total diatom

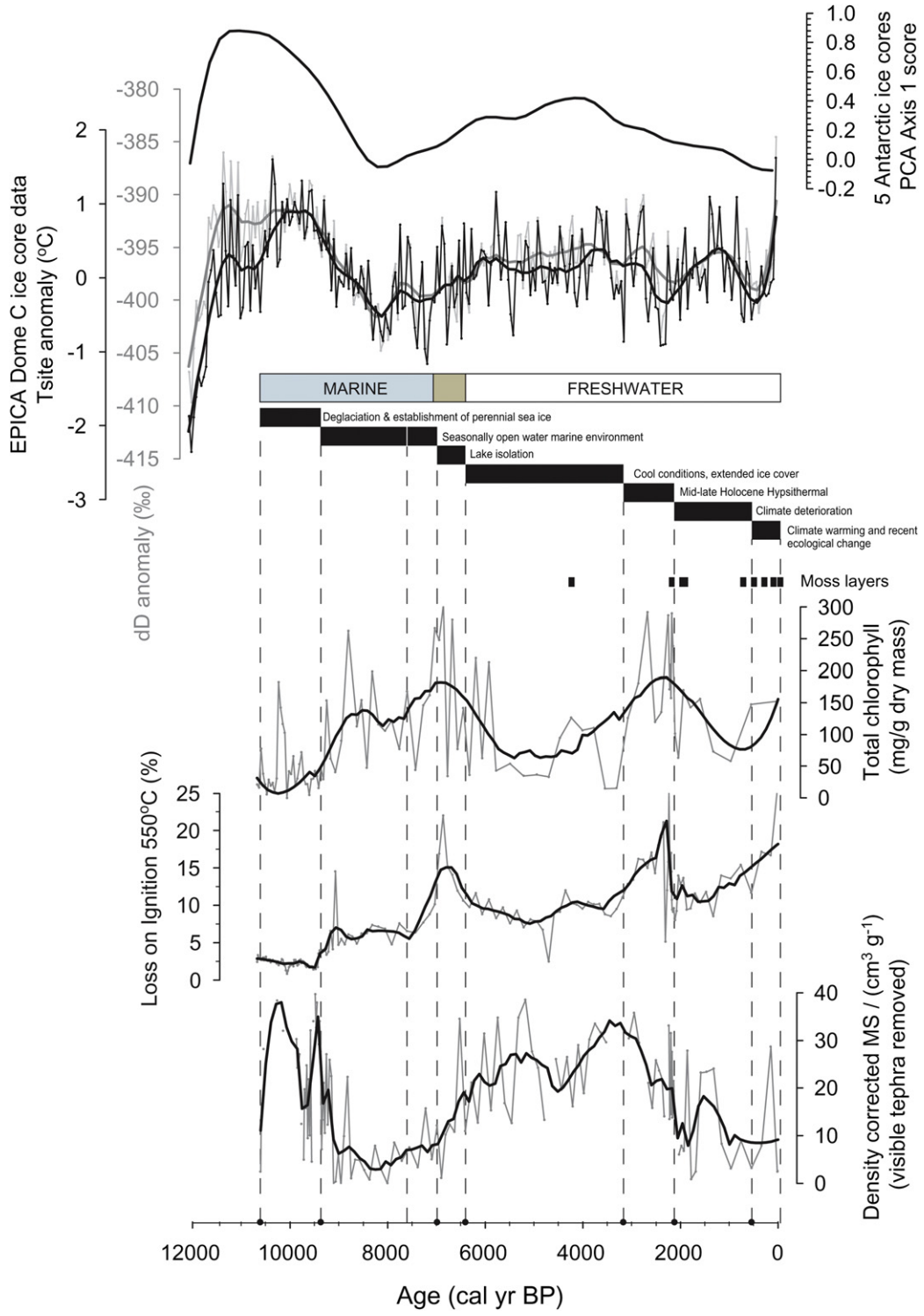

Fig. 7. Summary diagram showing selected palaeoenvironmental proxies from the Beak Lake 1 record, together with a synthesis of the main environmental changes interpreted from the core analyses (horizontal bars). These are compared with the Antarctic EPICA Dome C ice core deuterium-based temperature reconstructions (Stenni et al., 2003) and a Principal Components Analysis (showing Axis 1) of the common and residual signals in 5 Antarctic $\delta^{18}O$ records (Masson-Delmotte et al., 2011). Data are smoothed using negative exponential local smoothing using a third-order polynomial regression and weights from a Gaussian density function with outliers rejected; sampling proportion 0.1 except for Total chlorophyll which is 0.3 due to the lower resolution of the data.

concentrations, the high concentration of broken valves, the low organic carbon values (LOI_{550}), the low water content, the high magnetic susceptibility, the high sedimentation rates, a lithology composed of coarse material of varied sizes, and two ^{14}C dates being out of stratigraphic order. They suggest that the deglaciation inferred at 10,602 cal yr BP was not just a transition from a grounded ice stream to a floating ice shelf, but that icebergs and sea ice were present in Prince Gustav Channel at this time. This interpretation is supported by the diatom communities in this zone, which, were mainly composed of sea ice indicator taxa (*Navicula glaciei*;

Whitaker and Richardson, 1980) and thus likely reflect the presence of a nearly permanent, or at least seasonal sea ice cover over the coring site (e.g., Burckle and Cirilli, 1987). This interpretation does not rule out the presence of decaying icebergs, which can penetrate through pack-ice (Reece, 1950; Pudsey and Evans, 2001). The presence of some freshwater diatoms and cyanobacterial pigments (and possibly the older dates) is consistent with the incorporation of minor quantities of reworked freshwater or sub aerial sediments, presumably present in the basin or its environs prior to the early Holocene marine transgression.

5.2. 9372 to 6988 cal. BP: seasonally open water marine environment

From 9372–6988 cal yr BP (Diatom Zone 2, 105–76 cm) relatively productive, open water conditions influenced by seasonal meltwater were inferred. This is reflected in the higher organic content (LOI_{550}) values and increases in total diatom and pigment concentrations, all of which increased through this period. Diatom species richness and absolute abundances, mainly driven by CRS, reached their maxima. CRS are often found in open water assemblages, where surface waters are strongly stratified due to the melting of nearby ice (Karl et al., 1991; Buffen et al., 2007; Crosta et al., 2008). They typically occur in high productivity zones, with diverse phytoplankton assemblages (Comiso et al., 1990; Smith and Nelson, 1990; Leventer, 1992). Highly productive open water conditions were further supported by good pigment preservation including peaks in total pigment concentrations at 98 and 90 cm depth. Alloxanthin-like pigments were also resolved at 108 cm depth indicating the presence of cryptophytes (Jeffrey et al., 1997; Buchaca and Catalan, 2007), which have been associated with the increased meltwater runoff and reduced surface water salinities caused by the recent regional warming along the western AP margin (Moline et al., 2004). The reduction in coarse-grained debris and the slower sedimentation rates likely reflect the continued retreat of glaciers and ice shelves in the region and, a reduction in the number of (debris laden) icebergs.

In the upper part of Diatom Zone 2 (90–76 cm, 8746–6988 cal yr BP) total diatom concentrations peaked, together with a fucoxanthin derivative, and the species composition changed to nearshore marine and brackish-water taxa (e.g. *Craspedostauros* sp., *Navicula cryptotenella* and different *Nitzschia* species), sea ice and ice-melt related species (e.g., *Navicula glaciei*) and several ice-edge species (e.g., *Fragilariopsis cylindrus*). These shifts in diatom and pigment assemblages suggest that the basin was only isolated by a shallow sill. Under such circumstances regular flushing by sea water would be reduced, particularly in winter when ice may have grounded on the sill, and the basin may have experienced a combination of open sea water, winter sea ice, and brackish conditions following seasonal inflows of meltwater.

The period between 9372 and 6988 cal yr BP is not well resolved in AP palaeoenvironmental records, with contrasting patterns in the timing and duration of events (Bentley et al., 2009). This variability may reflect the shift from a regime strongly influenced by atmospheric warming (as seen in the ice cores from 11 000 to 9500 yr BP, Fig. 7), to one influenced by a combination of atmospheric and oceanographic forcing. Along the southwestern margin of the AP, there is evidence for the collapse of the King George VI Ice Shelf (Alexander Island) between c. 9600 and 7730 cal yr BP due to a combination of these forcings (Bentley et al., 2005; Smith et al., 2007) and for glacier thinning and ice margin retreat until at least 7200 yr BP (Bentley et al., 2006). This continued deglaciation coincides with the first part of what is termed a 'climate optimum' in the Palmer Deep record between 9070 and 3360 cal yr BP (Domack, 2002), which is likely to be associated, not with a geographically extensive atmospheric optimum (as this would be resolved in ice cores), but with a marine optimum, most likely due to the enhanced influx of warm circumpolar deep water onto the western AP continental shelf (cf. Smith et al., 2007), or a change in local atmospheric circulation reducing the extent of local sea ice (cf. Turner et al., 2009; p. 241). Similarly, a marine sediment core from Maxwell Bay (South Shetland Islands) recorded minimum sea ice densities and inferred warmer water between 8200 and 5900 cal yr BP (Milliken et al., 2009), but interestingly this was not supported by organic carbon measurements which did not increase until the Mid-late Holocene. Our record is also consistent with warmer but variable oceanographic conditions, and agrees with a recent study (A. Haworth, pers. comm.) on diatoms from southern Prince Gustav Channel, which suggests longer periods of seasonally open water conditions at the ice shelf edge occurred from around 8360 cal yr BP. On northern James Ross Island these warmer ocean conditions may have led to an increase in water availability and precipitation which could explain the local glacier readvance in Croft Bay and Brandy Bay (Fig. 1b, 9) between 7300 and 6700 ^{14}C BP (c. 8175–7960 and 7600–7430 cal yr BP) (Ingólfsson et al., 1992), although these initial findings were later revised to a shorter period of readvance into Brandy Bay between 5000 and 4500 ^{14}C yr BP (c. 5590–5890 and 4870–5290 cal yr BP) (Hjort et al., 1997, p.271).

5.3. 6988 to 6407 cal yr BP: lake isolation

The transition between marine, brackish and freshwater diatoms in Zone 3 was complete by 76 cm at 6988 cal yr BP, with freshwater diatoms dominant after 6407 cal yr BP (70 cm). This transition was the result of the isolation of the lake basin due to a fall in relative sea level, which we have described in detail elsewhere (Roberts et al., 2011). This isolation event dominated all proxies and prevents the reconstruction of past climate changes in this zone (cf. Wasell and Håkansson, 1992; Verleyen et al., 2004a,b). The transition accounts for the short peaks in diatom turnover and species richness and is dominated by diatoms, that are generally found in coastal lakes influenced by sea birds and mammals (e.g., the *N. frustulum/inconspicua* complex, *Nitzschia perminuta* and *N. seminulum*; Björck et al., 1996; Van de Vijver et al., 2008). The relatively high organic carbon content (LOI_{550}), increases in C/N and total diatom concentrations point to high productivity conditions due to the continued availability of a marine derived nutrient pool. Pigments respond earlier to the transition and their concentrations were highly variable with an increase in the number of degradation products consistent with a rapid succession of phototrophic communities responding to the changing environmental conditions.

Although the isolation event overrides other environmental changes, regionally this period coincides with relatively warm conditions reported in the Bransfield Basin between 6800 and 5900 cal yr BP (Heroy et al., 2007), maximal productivity near the inner Larsen-A region (Fig. 1) at c. 6300 ± 500 yr BP where ice shelf margin and open water conditions were present across the inner-middle shelf (Brachfeld et al., 2003; Evans et al., 2005) and the deglaciation of Hope Bay, ca 6300 ^{14}C yr BP (6735–7471 cal yr BP (Zale, 1994b) and its occupation by penguins sometime after c. 5500 cal yr BP (Zale, 1994a).

5.4. 6407 to 3169 cal yr BP: cool conditions with extended ice cover

The period between 6407 and 3169 cal yr BP (70–44 cm) shared identical diatom and pigment zone boundaries and was characterized by a decline in organic content (LOI_{550}) and total diatom and pigment concentrations. In some samples carotenoids were below detection limits. The diatom assemblages included increases in

Achnanthidium cf. *exiguum* and *B. minor*, species typical of high-altitude, nutrient-poor lakes on Livingston Island with low chlorophyll *a* concentrations (Jones and Juggins, 1995). Collectively these proxies suggest that cooler climate conditions had become established with more prolonged seasonal, or perennial, ice cover.

The onset of these cooler conditions predates the low nutrients and productivity inferred from an extensive growth of aquatic mosses in Lake Boeckella (Hope Bay) after 4700 cal yr BP (Gibson and Zale, 2006). However, its onset is nearly coeval with the onset of cold and arid climatic conditions inferred between c. 5890–5600 and 4840–4520 cal yr BP (c. 5000 and 4200 ^{14}C yr BP) from lake sediment cores on James Ross Island (Björck et al., 1996), which may have led to the glacier advances inferred on James Ross Island after c. 5450–4980 cal yr BP (4600 ^{14}C BP); although the latter paper links the glacial advances to a milder but more humid climate (Hjort et al., 1997) whereas the Beak Island record, which is independent of local glacier activity suggests that cold conditions may have induced the regional glacier advances during this period. In Maxwell Bay, in the South Shetland Islands a gradual oceanic cooling is inferred between 5900 and 2600 cal yr BP (Milliken et al., 2009).

5.5. 3169–2120 cal yr BP: Mid-late Holocene Hypsithermal

The period between is 3169 and 2120 cal yr BP (44–20 cm) was characterized by a prolonged peak in organic carbon content, total pigment concentrations (Fig. 7) and an increase in sediment accumulation rates. Interestingly the total diatom concentrations remained near stable which suggest that this period of higher primary production was dominated by other organisms including green algae, yellow-green algae and cyanobacteria (e.g., lutein, zeaxanthin, vaucheriaxanthin-like; Fig. 6) representing an increase in the diversity of the phototrophic community. The reappearance of phaeophorbide *a* is likely related to increased grazing activity by zooplankton and the development of a planktonic community; the latter being supported by the sub-dominance of the tychoplanktonic diatom species *S. pinnata*. The presence (although in small numbers) of some typical aerophilic diatoms could be associated with the development of moss communities like those present on the north-western shores of the lake, fed by small, braided meltwater streams. The presence of *Euglypha* type plates in this zone could corroborate this interpretation, pointing to moss growth in the catchment or littoral area of the lake (Vincke et al., 2006; Douglas and Smol, 2001). The near dominance of alloxanthin towards the top of this zone suggests that this period ended with major cryptophyte blooms. Collectively this period is consistent with a warmer climate and longer ice-free periods.

This period of increased primary productivity in Beak coincides with a period of increased diatom abundance in southern Prince Gustav Channel from 4270 to 3530 cal yr BP towards a peak between 2840 and 1340 cal yr BP (Haworth et al., pers. comm.). It is likely an expression of the Mid-late Holocene Hypsithermal (MHH), a warm period found in several parts of the AP and elsewhere in Antarctica (Hodgson et al., 2004; Verleyen et al., 2011). The exact timing of this event is however still inadequately resolved around the continent (Hodgson et al., 2009). At nearby James Ross Island it is seen in lake sediment records between c. 4680 and 3120 cal yr BP (4000 and 3000 ^{14}C yr BP; Björck et al., 1996), although the dating resolution of this study is limited to 2-3 radiocarbon dates per core. Better-dated records (14 radiocarbon dates) west of the Antarctic Peninsula, in the South Shetland Islands date the MHH at c. 4380–2530 with an optimum slightly after 3120 cal yr BP (4000–2500 and 3000 ^{14}C yr BP; Björck et al., 1993).

Similarly, to the north in the South Orkney Islands well-dated records (13–16 radiocarbon dates) place the MHH between 3800 and 1400 cal yr BP (Jones et al., 2000; Hodgson and Convey, 2005). This suggests that the onset of warming at Beak Island was buffered by the cooler climate systems of the Weddell Sea Gyre to the east of the Peninsula. Less precisely dated (due to marine reservoir effects) evidence for a warm period along the eastern margin of the AP suggests a previous collapse of the Prince Gustav Channel Ice Shelf further South in the Prince Gustav Channel ending at c. 1900 ^{14}C BP, when the ice shelf reformed (Pudsey & Evans, 2001), and in the Larsen-A region, fluctuations in ice shelf stability/extent were recorded at c. 3800, 2100 and 1400 yr BP (Brachfeld et al., 2003). Interestingly, this warm period postdates the maximum Holocene warming seen in ice cores from the continental plateau (Fig. 7).

5.6. 2120 to 543 cal yr BP: climate deterioration

From 2120 cal yr BP there was a marked decline in total pigment concentrations and a return to lower organic content. A rise in *B. minor* and *Psammothidium abundans*, which are typically associated with low nutrients, and the low carbonate content (LOI_{950}) might indicate more acidic conditions, associated with the establishment of benthic mosses which can have an acidifying influence on their direct environment (Wetzel, 2001) and which have been used as indicators of low productivity and low nutrient conditions in similar lakes in the AP region (Gibson and Zale, 2006). Alternatively, *B. minor*, which elsewhere is found in terrestrial moss habitats, may have been washed in from the marginal moss banks.

This period of low pigment concentrations, low nutrient conditions and possible acidity in the lake starting 2120 cal yr BP is interpreted as a climate cooling signal but slightly predates reconstructions in other regions of the AP, where a neoglacial cooling is only inferred for the past 1500 years (see Bentley et al., 2009). This earlier onset can possibly be attributed to the cooling effect of the Weddell Sea Gyre and corresponds with the reformation of ice shelves in the Prince Gustav Channel (1900 ^{14}C BP; Pudsey and Evans, 2001). In its later phase it is also consistent with the ice shelf stability recorded in the Larsen-A region after 1400 yr BP (Brachfeld et al., 2003), as well as neoglacial cooling in other parts of the AP (e.g. the South Shetland Islands: Björck et al., 1991a, 1993; and Bransfield Strait: Fabrés et al., 2000) and east Antarctica (Verleyen et al., 2011).

5.7. 543 cal yr BP to present: climate warming and recent ecological changes

A number of changes occurred in the top c. 5 cm which consisted of the most recent flocculent sediments together with abundant moss shoots. These included a lower wet density, a marked peak in organic content (LOI_{550}; Fig. 4), an increase in diatom species richness and an increase in species favoring moderately high nutrient concentrations (e.g. *Nitzschia frustulum/inconspicua*). For the diatoms a higher resolution analysis is required to determine the statistical significance of this change (Tavernier et al. unpubl. data). Similarly the response in the pigments is less clear due to the limited dry weight of material available for analysis. Nevertheless the positive shift in organic content, diatom species richness and changing diatom species composition occurred sometime after 543 cal yr BP. In its later phase above 3 cm, this warming signal may be associated with the measured increases in summer temperature at nearby Hope Bay of +0.41 °C per decade between 1946 and 2006 (Turner et al., 2009). Similar recent temperature rises have been recorded elsewhere in the AP (Vaughan et al., 2003; Bentley et al., 2009), and elsewhere in Antarctica (Hodgson et al., 2006b). This temperature increase has already affected the physical environment of the AP being linked to the recent recession of snowfields

and glaciers (Cook et al., 2005), a reduction in the duration of sea ice cover (Parkinson, 2002) and the disintegration of ice shelves (e.g., Vaughan and Doake, 1996; Rott et al., 1998; Scambos et al., 2003, Hodgson, 2011). This sediment core from Beak Island is amongst the first records to show a lacustrine response to this most recent period of rapid warming within a long-term historical context beyond instrumental records (cf. Quayle et al., 2002). It therefore mirrors similar studies in the Arctic where the temperature rises since the industrial revolution have resulted in significant regime shifts in lake ecosystems (e.g., Smol et al., 2005; Smol and Douglas, 2007).

6. Conclusions

This study has provided new well-dated multi proxy constraints on Holocene climate and environmental changes at Beak Island in the Prince Gustav Channel region north of James Ross Island. These include:

1. Establishing a minimum age for deglaciation of the study site of 10,602 cal yr BP from the presence of marine sediments and sea ice diatoms. This is similar to the minimum age of 10,605 cal yr BP measured on foraminifera in a marine sediment core on the inner continental shelf of the north-western Weddell Sea and with geomagnetic intensity ages of 10,700 $\pm$ 700 from the inner Larsen-A Ice Shelf region, suggesting a broadly synchronous disintegration of the north eastern part of the Antarctic Peninsula Ice Sheet at this time. Reconstructions of relative sea level change at Beak Island support this early Holocene deglaciation.
2. Evidence that the deglaciation post-dated the transition from a grounded ice stream to a floating ice shelf in Prince Gustav Channel, because iceberg rafted debris and sea ice diatoms were present in the Beak Lake1 sediment record from 10,602 cal yr BP.
3. Identifying a transition from nearly permanent sea ice cover and high iceberg concentrations to a seasonally open marine environment around 9372 cal yr BP. This broadly corresponds with the early retreat and disintegration of the ice shelf in southern Prince Gustav Channel.
4. Inferring relatively cool climate conditions between 6407 and 3169 cal yr BP.
5. Constraining the local timing of the Mid-late Holocene climate optimum to between 3169 and 2120 cal yr BP based on indicators of biological production. This onset postdates the onset of the MHH in the South Shetland Islands (4380 cal yr BP) and the South Orkney Islands (3800 cal yr BP) suggesting that cooler conditions in the Weddell Sea Gyre to the east of the Peninsula may have buffered the onset of warming. The warm period coincides with a previous collapse of the Prince Gustav Channel Ice Shelf which ended at c. 1900 ^{14}C BP, when the ice shelf reformed, and fluctuations in ice shelf stability/extent in the Larsen-A region, which were recorded until c. 1400 yr BP.
6. Constraining the return of cooler climate conditions from 2120 to 543 cal yr BP from a decrease in lake production and comparing this with evidence for neoglacial cooling elsewhere in Antarctica.
7. Finding evidence of an increase in the lake's primary production after 543 cal yr BP and a shift in the diatom communities in the upper 3 cm, and relating this to the recent measured regional warming trend at Hope Bay. This is amongst the first records to show an initial warming from 543 cal yr BP, followed by a lacustrine response to the most recent period of rapid warming within a long-term historical context and will be the subject of further study.

Acknowledgements

This study was funded by the UK Natural Environment Research Council through the British Antarctic Survey CACHE-PEP project (led by D.A. Hodgson) and the Belgian Science Policy Office project HOLANT (led by W. Vyverman). E. Verleyen is a postdoctoral research fellow of the Fund for Scientific Research Flanders, Belgium. Andy Lole is thanked for his assistance in the field and the captain and crew of the HMS Endurance and and 815 Naval Air Squadron for logistic support. Dr. Chris Hayward at the University of Edinburgh Tephrochronological Analytical Unit (TAU) is thanked for his assistance in undertaking preliminary microprobe analysis on the three main visible ash layers in this core, which will be the focus of a forthcoming paper.

Appendix. Supplementary data

Supplementary data related to this article can be found online at doi:10.1016/j.quascirev.2011.10.017.

References

Armand, L., Crosta, X., Romero, O., Pichon, J.J., 2005. The biogeography of major diatom taxa in southern ocean sediments. 1. Sea ice related species. Palaeogeography, Palaeoclimatology, Palaeoecology 223, 93–126.
Barcena, M.A., Fabrés, J., Isla, E., Flores, J.A., Sierro, F.J., Canals, M., Palanques, A., 1998. Holocene neoglacial events in the Bransfield Strait (Antarctica). Palaeocenographic and palaeoclimatic significance. Scientia Marina 70, 607–619.
Battarbee, R.W., Kneen, M., 1982. The use of electronically counted microspheres in absolute diatom analysis. Limnology and Oceanography 27, 184–188.
Bennett, K.D., 1996. Determination of the number of zones in a biostratigraphical sequence. New Phytologist 132, 155–170.
Bentley, M.J., Hodgson, D.A., Sugden, D.E., Roberts, S.J., Smith, J.A., Leng, M.J., Bryant, C., 2005. Early Holocene retreat of the George VI ice shelf, Antarctic Peninsula. Geology 33, 173–176.
Bentley, M.J., Fogwill, C.J., Kubik, P.W., Sugden, D.E., 2006. Geomorphological evidence and cosmogenic 10Be/26Al exposure ages for the Last Glacial Maximum and deglaciation of the Antarctic Peninsula ice sheet. Geological Society of America Bulletin 118, 1149–1159.
Bentley, M.J., Hodgson, D.A., Smith, J.A., Ó Cofaigh, C., Domack, E.W., Larter, R.D., Roberts, S.J., Brachfeld, S., Leventer, A., Hjort, C., Hillenbrand, C.-D., Evans, J., 2009. Mechanisms of Holocene palaeoenvironmental change in the Antarctic Peninsula region. The Holocene 19, 51–69.
Bibby, J.S., 1966. The stratigraphy of part of north-east Graham land and the James Ross island group. Scientific Reports 53, 1–37. British Antarctic Survey.
Björck, S., Håkansson, H., Zale, R., Karlén, W., Jönssen, B.L., 1991a. A late Holocene lake sediment sequence from Livingston island, south Shetland islands, with palaeoclimatic implications. Antarctic Science 3 (1), 61–72.
Björck, S., Hjort, C., Ingólfsson, O., Skog, G., 1991b. Radiocarbon dates from the Antarctic Peninsula – problems and potential. Quaternary Proceedings. In: Lowe, J.J. (Ed.), Radiocarbon Dating: Recent Applications and Future Potential. Quaternary Research Association, Cambridge, pp. 55–65.
Björck, S., Sandgren, P., Zale, R., 1991c. Late Holocene tephrochronology of the northern Antarctic Peninsula. Quaternary Research 36, 322–328.
Björck, S., Håkansson, H., Olssen, S., Banekow, L., Janssens, J., 1993. Palaeoclimatic studies in south Shetland islands, Antarctica, based on numerous stratigraphic variables in lake sediments. Journal of Paleolimnology 8, 233–272.
Björck, S., Olsson, S., Ellis-Evans, C., Håkansson, H., Humlum, O., de Lirio, J.M., 1996. Late Holocene palaeoclimatic records from lake sediments on James Ross island, Antarctica. Palaeogeography, Palaeoclimatology, Palaeoecology 121, 195–220.
Blaauw, M., 2010. Methods and code for 'classical' age-modelling of radiocarbon sequences. Quaternary Geochronology 5, 512–518.
Brachfeld, S., Domack, E., Kissel, C., Laj, C., Leventer, A., Ishman, S., Gilbert, R., Camerlenghi, A., Eglinton, L.B., 2003. Holocene history of the Larsen-A ice shelf constrained by geomagnetic paleointensity dating. Geology 31, 749–752.
Bronk Ramsey, C., 2001. Development of the radiocarbon calibration program OxCal. Radiocarbon 43 (2A), 355–363.
Buchaca, T., Catalan, J., 2007. Factors influencing the variability of pigments in the surface sediments of mountain lakes. Freshwater Biology 52, 1365–1379.
Buffen, A., Leventer, A., Rubin, A., Hutchins, T., 2007. Diatom assemblages in surface sediments of the northwestern Weddell sea, Antarctic Peninsula. Marine Micropaleontology 62, 7–30.
Burckle, L.H., Cirilli, J., 1987. Origin of diatom ooze belt in the southern-ocean – implications for late Quaternary Paleoceanography. Micropaleontology 33, 82–86.
Comiso, J.C., Maynard, N.G., Smith, W.O., Sullivan, C.W., 1990. Satellite ocean color studies of Antarctic ice edges in summer and autumn. Journal of Geophysical Research-Oceans 95, 9481–9496.

Cook, A.J., Fox, A.J., Vaughan, D.G., Ferrigno, J.G., 2005. Retreating glacier fronts on the Antarctic Peninsula over the past half-century. Science 308, 541–544.
Cremer, H., Roberts, D., McMinn, A., Gore, D., Melles, M., 2003. The Holocene diatom flora of marine bays in the Windmill islands, east Antarctica. Botanica Marina 43, 82–106.
Cremer, H., Gore, D., Hultzsch, N., Melles, M., Wagner, B., 2004. The diatom flora and limnology of lakes in the Amery Oasis, east Antarctica. Polar Biology 27, 513–531.
Crosta, X., Denis, D., Ther, O., 2008. Sea ice seasonality during the Holocene, Adelie land, east Antarctica. Marine Micropaleontology 66, 222–232.
De Angelis, H., Skvarca, P., 2003. Glacier Surge after ice shelf collapse. Science 299, 1560–1562.
Dean, W.E., 1974. Determination of carbonate and organic-matter in Calcareous sediments and sedimentary-rocks by loss on ignition – comparison with other methods. Journal of Sedimentary Petrology 44, 242–248.
Domack, E.W., 2002. A synthesis for site 1098: palmer deep. available online:. In: Barker, P.F., Camerlenghi, A., Acton, G.D., Ramsay, A.T.S. (Eds.), Proceedings of ODP Scientific Results 178, pp. 1–14 http://www-odp.tamu.edu/publications/178_SR/VOLUME/CHAPTERS/SR178_34.pdf [2008-10-03].
Domack, E., Duran, D., Leventer, A., Ishman, S., Doane, S., Mccallum, S., Amblas, D., Ring, J., Gilbert, R., Prentice, M., 2005. Stability of the Larsen B ice shelf on the Antarctic Peninsula during the Holocene Epoch. Nature 436, 681–685.
Douglas, M.S.V., Smol, J.P., 1995. Paleolimnological significance of observed distribution patterns of chrysophyte cysts in arctic pond environments. Journal of Paleolimnology 13, 1–5.
Douglas, M.S.V., Smol, J.P., 2001. Siliceous protozoan plates and scales (Chapter 13). In: Smol, J.P., Birks, H.J.B., Last, W.M. (Eds.), Tracking Environmental Change Using Lake Sediments. Terrestrial, Algal, and Siliceous Indicators, vol. 3. Kluwer Academic Publishers, Dordrecht, pp. 265–279.
Evans, J., Pudsey, C.J., Ó Cofaigh, C., Morris, P., Domack, E., 2005. Late Quaternary glacial history, flow dynamics and sedimentation along the eastern margin of the Antarctic Peninsula ice sheet. Quaternary Science Reviews 24, 741–774.
Fabrés, J., Calafat, A.M., Canals, M., Bárcena, M.A., Flores, J.A., 2000. Bransfield basin fine grained sediments: Late Holocene sedimentary processes and oceanographic and climatic conditions. Holocene 10 (9), 703–718.
Fretzdorff, S., Smellie, J., 2002. Electron microprobe characterization of ash layers in sediments from the central Bransfield basin (Antarctic Peninsula): evidence for at least two volcanic sources. Antarctic Science 14 (4), 412–421.
Gibson, J.A.E., Zale, R., 2006. Holocene development of the fauna of lake Boeckella, northern Antarctic Peninsula. Holocene 16, 625–634.
Grimm, E.C., 1987. CONISS – a Fortran-77 program for stratigraphically constrained cluster-analysis by the method of Incremental sum of Squares. Computers & Geosciences 13, 13–35.
Grimm, E.C., 1991–1993. Tilia 2.0 Version b.4 and TiliaGraph. Ilinois State Museum, Springfield, Ilinois.
Grimm, E.C., 2004. TGView Version 2.0.2. Illinois State Museum, Springfield, Ilinois.
Heroy, D.C., Anderson, J.B., 2007. Radiocarbon constraints on Antarctic Peninsula ice sheet retreat following the Last Glacial Maximum (LGM). Quaternary Science Reviews 26, 3286–3297.
Heroy, D.C., Sjunneskog, C., Anderson, J.B., 2007. Holocene climate change in the Bransfield basin, Antarctic Peninsula: evidence from sediment and diatom analysis. Antarctic Science. doi:10.1017/S0954102007000788.
Hjort, C., Ingólfsson, Ó, Möller, P., Lirio, J.M., 1997. Holocene glacial history and sea-level changes on James Ross Island, Antarctic Peninsula. Journal of Quaternary Science 12 (4), 259–273.
Hjort, C., Ingólfsson, Ó, Bentley, M.J., Björck, S., 2003. The late Pleistocene and Holocene glacial and climate history of the Antarctic Peninsula region as documented by the land and lake sediment records – a review. Antarctic Research Series 79, 95–102.
Hodgson, D.A., Convey, P., 2005. A 7000-Year record of Oribatid Mite communities on a Maritime-Antarctic island: responses to climate change. Arctic Antarctic and Alpine Research 37, 239–245.
Hodgson, D.A., Dyson, C.L., Jones, V.J., Smellie, J.L., 1998. Tephra analysis of sediments from Midge lake (South Shetland Islands) and Sombre lake (South Orkney Islands), Antarctica. Antarctic Science 10 (1), 13–20.
Hodgson, D.A., Vyverman, W., Sabbe, K., 2001. Limnology and Biology of saline lakes in the Rauer Islands, eastern Antarctica. Antarctic Science 13, 255–270.
Hodgson, D.A., Doran, P., Roberts, D., McMinn, A., 2004. Paleolimnological studies from the Antarctic and subantarctic islands. In: Pienitz, R., Douglas, S.V., Smol, J.P. (Eds.), Long-term Environmental Change in Arctic and Antarctic Lakes. Springer, Dordrecht, pp. 419–474.
Hodgson, D.A., Bentley, M.J., Roberts, S.J., Smith, J.A., Sugden, D.E., Domack, E.W., 2006a. Examining Holocene stability of Antarctic Peninsula ice shelves. Eos Transactions, American Geophysical Union 87, 305–312.
Hodgson, D.A., Roberts, D., McMinn, A., Verleyen, E., Terry, B., Corbett, C., Vyverman, W., 2006b. Recent rapid salinity rise in three east Antarctic lakes. Journal of Paleolimnology 36, 385–406.
Hodgson, D.A., Abram, N., Anderson, J., Bargelloni, L., Barrett, P., Bentley, M.J., Bertler, N.A.N., Chown, S., Clarke, A., Convey, P., Crame, A., Crosta, X., Curran, M., di Prisco, G., Francis, J.E., Goodwin, I., Gutt, J., Massé, G., Masson-Delmotte, V., Mayewski, P.A., Mulvaney, R., Peck, L., Pörtner, H.-O., Röthlisberger, R., Stevens, M.I., Summerhayes, C.P., van Ommen, T., Verde, C., Verleyen, E., Vyverman, W., Wiencke, C., Zane, L., 2009. Antarctic climate and environment history in the pre-instrumental period. In: Turner, J., Convey, P., di Prisco, G., Mayewski, P.A., Hodgson, D.A., Fahrbach, E., Bindschadler, R., Gutt, J. (Eds.), Antarctic Climate Change and the Environment. Scientific Committee for Antarctic Research, Cambridge, pp. 115–182.
Hodgson, D.A., Roberts, S.J., Bentley, M.J., Smith, J.A., Johnson, J.S., Verleyen, E., Vyverman, W., Hodson, A.J., Leng, M.J., Cziferszky, A., Fox, A.J., Sanderson, D.C.W., 2009b. Exploring former subglacial Hodgson lake. Paper I: site description, geomorphology and limnology. Quaternary Science Reviews 28, 2295–2309.
Hodgson, D.A., 2011. First synchronous retreat of ice shelves marks a new phase of polar deglaciation. Proceedings of the National Academy of Sciences, USA, doi:10.1073/pnas.1116515108
Houghton, J.T., Ding, Y., Griggs, D.J., Noguer, M., van der Linden, P.J., Dai, X., Maskell, K., Johnson, C.A., 2001. Climate change 2001: the scientific basis. In: Contribution of Working Group I to the Third Assessment Report of the Intergovernmental Panel on Climate Change. Cambridge University Press, New York.
Hua, Q., Barbetti, M., 2004. Review of tropospheric bomb C-14 data for carbon cycle modeling and age calibration purposes. Radiocarbon 46, 1273–1298.
Ingólfsson, O., Hjort, C., Björck, S., Smith, R.I.L., 1992. Late Pleistocene and Holocene glacial history of James-Ross-Island, Antarctic Peninsula. Boreas 21, 209–222.
Ingólfsson, O., Hjort, C., Humlum, O., 2003. Glacial and climate history of the Antarctic Peninsula since the Last Glacial Maximum. Arctic Antarctic and Alpine Research 35, 175–186.
Jeffrey, S.W., Mantoura, R.F.C., Bjornland, T., 1997. Data for the identification of 47 key phytoplankton pigments. In: Jeffrey, S.W., Mantoura, R.F.C., Wright, S.W. (Eds.), Phytoplankton Pigments in Oceanography, Guidelines to Modern Methods. Monographs on Oceanographic Methodology (SCOR), vol. 10. UNESCO Publishing, pp. 447–554.
Johnson, J.S., Bentley, M.J., Roberts, S.J., Binnie, S.A., Freeman, S., 2011. Holocene deglacial history of the north east Antarctic Peninsula. Quaternary Science Reviews 30, 3791–3802.
Jones, V.J., Juggins, S., 1995. The Construction of a diatom-based chlorophyll a transfer function and its application at three lakes on Signy island (Maritime Antarctic) subject to differing degrees of nutrient enrichment. Freshwater Biology 34, 433–445.
Jones, V.J., Juggins, S., Ellis-Evans, J.C., 1993. The relationship between water Chemistry and surface sediment diatom assemblages in Maritime Antarctic lakes. Antarctic Science 5, 339–348.
Jones, V.J., Hodgson, D.A., Chepstow-Lusty, A., 2000. Palaeolimnological evidence for marked Holocene environmental changes on Signy Island, Antarctica. The Holocene 10 (1), 43–60.
Juggins, S. (2009). Rioja, analysis of Quaternary science data. http://www.staff.ncl.ac.uk/staff/stephen.juggins/.
Karl, D.M., Tilbrook, B.D., Tien, G., 1991. Seasonal coupling of organic matter production and particle flux in the Antarctic Peninsula region. Deep-Sea Research 38, 1097–1126.
Leavitt, P.R., Findlay, D.L., 1994. Comparison of fossil pigments with 20 years of phytoplankton data from Eutrophic Lake-227, Experimental lakes area, Ontario. Canadian Journal of Fisheries and Aquatic Sciences 51, 2286–2299.
Leavitt, P.R., Hodgson, D.A., 2001. Sedimentary pigments. In: Smol, J.P., Last, W.S. (Eds.), Developments in Palaeoenvironmental Research. Tracking Environmental Changes Using Lake Sediments, Biological Techniques and Indicators, vol. 3. Kluwer, pp. 295–325.
Lee, Y.I., Limb, H.S., Yoon, H.I., Tatur, A., 2007. Characteristics of tephra in Holocene lake sediments on king George island, west Antarctica: implications for deglaciation and paleoenvironment. Quaternary Science Reviews 26, 3167–3178.
Leventer, A., 1992. Modern distribution of diatoms in sediments from the George-V-Coast, Antarctica. Marine Micropaleontology 19, 315–332.
Masson-Delmotte, V., Stenni, B., Jouzel, J., 2004. Common millennial-scale variability of Antarctic and southern ocean temperatures during the past 5000 years reconstructed from the EPICA Dome C ice core. The Holocene 14, 145–151.
Masson-Delmotte, V., Buiron, D., Ekaykin, A., Frezzotti, M., Galĺee, H., Jouzel, J., Krinner, G., Landais, A., Motoyama, H., Oerter, H., Pol, K., Pollard, D., Ritz, C., Schlosser, E., Sime, L.C., Sodemann, H., Stenni, B., Uemura, R., Vimeux, F., 2011. A comparison of the present and Last Interglacial periods in six Antarctic ice cores. Climate of the Past 7, 397–423. doi:10.5194/cp-7-397-2011.
McCormac, F., Hogg, A., Blackwell, P., Buck, C., Higham, T., Reimer, P., 2004. Shcal04 southern Hemisphere calibration 0-11.0 cal kyr Bp. Radiocarbon 46, 1087–1092.
Milliken, K.T., Anderson, J.B., Wellner, J.S., Bohaty, S.M., Manley, P.L., 2009. High-resolution Holocene climate record from Maxwell Bay, south Shetland islands, Antarctica. Geological Society of America Bulletin 121 (11–12), 1711–1725.
Moline, M.A., Claustre, H., Frazer, T.K., Schofield, O., Vernet, M., 2004. Alteration of the Food Web along the Antarctic Peninsula in response to a regional warming trend. Global Change Biology 10, 1973–1980.
Mulvaney, R., Alemany, O., Possenti, P., 2007. The Berkner island (Antarctica) ice-core drilling project. Annals of Glaciology 47 (1), 115–124.
Narcisi, B., Petit, J.R., Delmonte, B., Basile-Doelsch, I., Maggi, V., 2005. Characteristics and sources of tephra layers in the EPICA-Dome C ice record (East Antarctica): implications for past atmospheric circulation and ice core stratigraphic correlations. Earth and Planetary Science Letters 239, 253–265.
Ó Cofaigh, C., Dowdeswell, J.A., Allen, C.S., Hiemstra, J.F., Pudsey, C.J., Evans, J., Evans, D.J.A., 2005. Flow dynamics and till genesis associated with a marine-based Antarctic palaeo-ice stream. Quaternary Science Reviews 24, 709–740.

Ochyra, R., 2008. Mosses of the Prince Edward islands. In: Chown, R.S., Froneman, P.W. (Eds.), Prince Edward Islands. Sun Press, Stellenbosch, South Africa, pp. 383–389.
Parkinson, C.L., 2002. Trends in the length of the southern ocean sea-ice season, 1979–99. 4th International Symposium on Remote Sensing (in Glaciology), Date: June 03-08, 2001. In: Winther, J.G., Solberg, R. (Eds.), Annals of Glaciology, vol. 34. Univ. Maryland College pk, Maryland, pp. 435–440.
Patrick, R., Reimer, C.W., 1966. The diatoms of the United States, exclusive of Alaska and Hawaii. Monograph No. 13. In: Volume 1-Fragilariaceae, Eunotiaceae, Achnanthaceae, Naviculaceae. Academy of Natural Sciences of Philadelphia, pp. 1–688.
Pudsey, C.J., Evans, J., 2001. First survey of Antarctic sub-ice shelf sediments reveals Mid-Holocene ice shelf retreat. Geology 29, 787–790.
Pudsey, C.J., Murray, J.W., Appleby, P., Evans, J., 2006. Ice shelf history from petrographic and foraminiferal evidence, northeast Antarctic Peninsula. Quaternary Science Reviews 25, 2357–2379.
Pushkar, V.S., Roof, S.R., Cherepanova, M.V., Hopkins, D.M., Brigham-Grette, J., 1999. Paleogeographic and Paleoclimatic significance of diatoms from middle Pleistocene marine and glaciomarine deposits on Baldwin Peninsula, northwestern Alaska. Palaeogeography, Palaeoclimatology, Palaeoecology 152, 67–85.
Quayle, W.C., Peck, L.S., Peat, H., Ellis-Evans, J.C., Harrigan, P.R., 2002. Extreme responses to climate change in Antarctic lakes. Science 295 645–.
Rabassa, J., 1983. Stratigraphy of the glacigenic deposits in northern James Ross island, Antarctic Peninsula. In: Evenson, E., Schlüchter, C., Rabassa, J. (Eds.), Tills and Related Deposits. A.A. Bakema Publishers, Rotterdam, pp. 329–340.
Reece, A., 1950. The ice of crown prince gustav channel, Graham land, Antarctica. Journal of Glaciology 1, 404–409.
Reimer, P.J., Reimer, R., 2011. CALIBomb Radiocarbon Calibration Program. http://calib.qub.ac.uk/CALIBomb/.
Reimer, P.J., Baillie, M.G.L., Bard, E., Bayliss, A., Beck, J.W., Bertrand, C.J.H., Blackwell, P.G., Buck, C.E., Burr, G.S., Cutler, K.B., Damon, P.E., Edwards, R.L., Fairbanks, R.G., Friedrich, M., Guilderson, T.P., Hogg, A.G., Hughen, K.A., Kromer, B., McCormac, G., Manning, S., Ramsey, C.B., Reimer, R.W., Remmele, S., Southon, J.R., Stuiver, M., Talamo, S., Taylor, F.W., Van Der Plicht, J., Weyhenmeyer, C.E., 2004a. Intcal04 terrestrial radiocarbon age calibration, 0–26 cal kyr BP. Radiocarbon 46, 1029–1058.
Reimer, P.J., Brown, T.A., Reimer, R.W., 2004b. Discussion: reporting and calibration of post-bomb ^{14}C data. Radiocarbon 46, 1299–1304.
Reimer, P.J., Baillie, M.G.L., Bard, E., Bayliss, A., Beck, J.W., Blackwell, P.G., Bronk Ramsey, C., Buck, C.E., Burr, G.S., Edwards, R.L., Friedrich, M., Grootes, P.M., Guilderson, T.P., Hajdas, I., Heaton, T.J., Hogg, A.G., Hughen, K.A., Kaiser, K.F., Kromer, B., McCormac, F.G., Manning, S.W., Reimer, R.W., Richards, D.A., Southon, J.R., Talamo, S., Turney, C.S.M., van der Plicht, J., Weyhenmeyer, C.E., 2009. IntCal09 and Marine09 radiocarbon age calibration curves, 0–50,000 years cal. BP. Radiocarbon 51, 1111–1150.
Renberg, I., 1990. A procedure for preparing large sets of diatom slides from sediment cores. Journal of Paleolimnology 4, 87–90.
Risso, C., Scasso, R.A., Aparicio, A., 2002. Presence of large pumice blocks on Tierra del Fuego and South Shetland Islands shorelines, from 1962 South Sandwich Islands eruption. Marine Geology 186, 413–422.
Roberts, D., McMinn, A., 1999. Diatoms of the saline lakes of the Vestfold Hills, Antarctica. Bibliotheca Diatomologica 44, 1–83.
Roberts, S.J., Hodgson, D.A., Bentley, M.J., Smith, J.A., Millar, I.L., Olive, V., Sugden, D.E., 2008. The Holocene history of George Vi ice shelf, Antarctic Peninsula from Clast-Provenance analysis of Epishelf lake sediments. Palaeogeography Palaeoclimatology Palaeoecology 259, 258–283.
Roberts, S.J., Hodgson, D.A., Sterken, M., Whitehouse, P.L., Verleyen, E., Vyverman, W., Sabbe, K., Balbo, A., Bentley, M.J., Moreton, S.G., 2011. Geological constraints on glacio-isostatic adjustment models of relative sea-level change during deglaciation of Prince Gustav Channel, Antarctic Peninsula. Quaternary Science Reviews 30, 3603–3617.
Rott, H., Rack, W., Nagler, T., Skvarca, P., 1998. Climatically induced retreat and collapse of northern Larsen ice shelf, Antarctic Peninsula. Annals of Glaciology 27, 86–92.
Round, F.E., Crawford, R.M., Mann, D.G., 1990. The Diatoms: Biology and Morphology of the Genera. Cambridge University Press, Cambridge.
Sabbe, K., Verleyen, E., Hodgson, D.A., Vanhoutte, K., Vyverman, W., 2003. Benthic diatom flora of freshwater and saline lakes in the Larsemann Hills and Rauer islands, east Antarctica. Antarctic Science 15, 227–248.
Scambos, T., Hulbe, C., Fahnestock, M., 2003. Climate-Induced ice shelf disintegration in the Antarctic Peninsula. Antarctic Peninsula climate variability: historical and Paleoenvironmental perspectives. International Workshop on Antarctic Peninsula Climate Variability, Date: April, 2002. Hamilton College Clinton, NY, vol. 79, pp. 79–92.
Scambos, T.A., Bohlander, J.A., Shuman, C.A., Skvarca, P., 2004. Glacier acceleration and thinning after ice shelf collapse in the Larsen B embayment, Antarctica. Geophysical Research Letters 31 (18) Art. n° L18402.
Sjunneskog, C., Taylor, F., 2002. Postglacial marine diatom record of the Palmer deep, Antarctic Peninsula (ODP Leg 178, site 1098) 1. Total diatom abundance. Paleoceanography 17 (3) Art. n° 8003.
Smellie, J.L., 1999. The upper Cenozoic tephra record in the south polar region: a review. Global and Planetary Change 21, 51–70.
Smellie, J.L., 2001. Lithostratigraphy and volcanic evolution of Deception Island, south Shetland Islands. Antarctic Science 13, 188–209.
Smith, H.G., 1992. Distribution and ecology of the testate rhizopod fauna of the continental Antarctic zone. Polar Biology 12, 629–634.
Smith, W.O., Nelson, D.M., 1990. Phytoplankton growth and new production in the Weddell sea marginal ice zone during austral spring and autumn. Limnology & Oceanography 35, 809–821.
Smith, J.A., Bentley, M.J., Hodgson, D.A., Roberts, S.J., Leng, M.J., Lloyd, J.M., Barrett, M.S., Bryant, C., Sugden, D.E., 2007. Oceanic and atmospheric forcing of early Holocene ice shelf retreat, George VI ice shelf, Antarctica Peninsula. Quaternary Science Reviews 26, 500–516.
Smith, J.A., Hillenbrand, C.-D., Pudsey, C.J., Allen, C.S., Graham, A.G.C., 2010. The presence of polynyas in the Weddell sea during the last glacial period with implications for the reconstruction of sea-ice limits and ice sheet history. Earth and Planetary Science Letters 296, 287–298.
Smol, J.P., 1983. Paleophycology of a high arctic lake near Cape Herschel, Ellesmere island. Canadian Journal of Botany 61, 2195–2204.
Smol, J.P., 1988. Chrysophycean microfossils in paleolimnological studies. Palaeogeography, Palaeoclimatology, Palaeoecology 62, 287–297.
Smol, J.P., Douglas, M.S.V., 2007. Crossing the final ecological threshold in high arctic ponds. Proceedings of the National Academy of Sciences 104 (30), 12395–12397.
Smol, J.P., Wolfe, A.P., Birks, H.J.B., Douglas, M.S.V., Jones, V.J., Korhola, A., Pienitz, R., Rühland, K., Sorvari, S., Antoniades, D., Brooks, S.J., Fallu, M.-A., Hughes, M., Keatley, E., Laing, T.E., Michelutti, N., Nazarova, L., Nyman, M., Paterson, A.M., Perren, B., Quinlan, R., Rautio, M., Saulnier-Talbot, E., Siitonen, S., Solovieva, N., Weckström, J., 2005. Climate-driven regime shifts in the biological communities of arctic lakes. Proceedings of the National Academy of Sciences 102 (12), 4397–4402.
Stenni, B., Jouzel, J., Masson-Delmotte, V., Röthlisberger, R., Castellano, E., Cattani, O., Falourd, S., Johnsen, S.J., Longinelli, A., Sachs, J.P., et al., 2003. A late-glacial high-resolution site and source temperature record derived from the EPICA Dome C isotope records (East antarctica). Earth and Planetary Science Letters 217, 183–195. 110.1016/S0012-1821X(1003)00574-00570.
Sterken M., Van de Vijver B., Jone V.J., Verleyen E., Hodgson D.A., Vyverman W., Sabbe K. An illustrated and annotated checklist of freshwater diatoms (Bacillariophyta) from the Maritime Antarctic (Livingston, Signy and Beak Island), submitted for publication.
Taylor, F., Sjunneskog, C., 2002. Postglacial marine diatom record of the Palmer deep, Antarctic Peninsula (ODP Leg 178, site 1098) 2. Diatom assemblages. Paleoceanography 17 (3) Art. N°8001.
Taylor, F., Whitehead, J., Domack, E., 2001. Holocene paleoclimate change in the Antarctic Peninsula: evidence from the diatom, sedimentary and geochemical record. Marine Micropaleontology 41 (1–2), 25–43.
Turner, J., Arthern, R., Bromwich, D., Marshall, G., Worby, T., Bockheim, J., di Prisco, G., Verde, C., Convey, P., Roscoe, H., Jones, A., Vaughan, D., Woodworth, P., Scambos, T., Cook, A., Lenton, A., Comiso, J., Gugliemin, M., Summerhayes, C., Meredith, M., Naveira-Garabato, A., Chown, S., Stevens, M., Adams, B., Worland, R., Hennion, F., Huiskes, A., Bergstrom, D., Hodgson, D.A., Bindschadler, R., Bargagli, R., Metzl, N., van der Veen, K., Monaghan, A., Speer, K., Rintoul, S., Hellmer, H., Jacobs, S., Heywood, K., Holland, D., Yamanouchi, T., Barbante, C., Bertler, N., Boutron, C., Hong, S., Mayewski, P., Fastook, J., Newsham, K., Robinson, S., Forcarda, J., Trathan, P., Smetacek, V., Gutt, J., Pörtner, H.-O., Peck, L., Gili, J.-M., Wiencke, C., Fahrbach, E., Atkinson, A., Webb, D., Isla, E., Orejas, C., Rossi, S., Shanklin, J., 2009. The instrumental period. In: Turner, J., et al. (Eds.), Antarctic Climate Change and the Environment. Scientific Committee for Antarctic Research, Cambridge, pp. 183–298.
Van de Vijver, B., Beyens, L., 1997. Freshwater diatoms from some islands in the Maritime Antarctic region. Antarctic Science 9, 418–425.
Van de Vijver, B., Frenot, Y., Beyens, L., 2002. Freshwater diatoms from Ile de la Possession (Crozet Archipelago, Subantarctica). Bibliotheca Diatomologica 46, 1–412.
Van de Vijver, B., Gremmen, N., Smith, V., 2008. Diatom communities from the sub-Antarctic Prince Edward islands: diversity and distribution patterns. Polar Biology 31 (7), 795–808.
Van de Vijver, B., Sterken, M., Vyverman, W., Mataloni, G., Nedbalova, L., Kopalova, K., Verleyen, E., Sabbe, K., 2010. Four new non-marine diatom taxa from islands in the southern Atlantic ocean. Diatom Research 25, 431–443.
Vaughan, D.G., 2006. Recent trends in melting conditions on the Antarctic Peninsula and their implications for ice-sheet mass balance. Arctic, Antarctic and Alpine Research 38, 147–152.
Vaughan, D.G., Doake, C.S.M., 1996. Recent atmospheric warming and retreat of ice shelves on the Antarctic Peninsula. Nature 379, 328–331.
Vaughan, D.G., Marshall, G.J., Connolley, W.M., Parkinson, C., Mulvaney, R., Hodgson, D.A., King, J.C., Pudsey, C.J., Turner, J., 2003. Recent rapid regional climate warming on the Antarctic Peninsula. Climatic Change 60, 243–274.
Verleyen, E., Hodgson, D.A., Vyverman, W., Roberts, D., McMinn, A., Vanhoutte, K., Sabbe, K., 2003. Modelling diatom responses to climate induced fluctuations in the moisture balance in continental Antarctic lakes. Journal of Paleolimnology 30 (2), 195–215.
Verleyen, E., Hodgson, D.A., Sabbe, K., Vanhoutte, K., Vyverman, W., 2004a. Coastal oceanographic conditions in the Prydz Bay region (East Antarctica) during the Holocene recorded in an isolation basin. The Holocene 14 (2), 246–257.
Verleyen, E., Hodgson, D.A., Sabbe, K., Vyverman, W., 2004b. Late Quaternary deglaciation and climate history of the Larsemann Hills (East Antarctica). Journal of Quaternary Science 19 (4), 361–375.
Verleyen, E., Hodgson, D.A., Sabbe, K., Cremer, H., Emslie, S.D., Gibson, J., Hall, B., Satoshi, I., Kudoh, S., Marshall, G.J., McMinn, A., Melles, M., Newman, L.,

Roberts, D., Roberts, S., Singh, S.M., Sterken, M., Tavernier, I., Verkulich, S., Van de Vyver, E., Van Nieuwenhuyze, W., Wagner, B., Vyverman, W., 2011. Post-glacial climate variability along the east Antarctic coastal margin – evidence from shallow marine and coastal terrestrial records. Earth Science Reviews 104 (4), 199–212.

Vincke, S., Van de Vijver, B., Gremmen, N., Beyens, L., 2006. The moss dwelling testacean fauna of the Stromness Bay (South Georgia). Acta Protozoologica 45, 65–75.

Wasell, A., Håkansson, H., 1992. Diatom stratigraphy in a lake on Horseshoe island, antarctica: a marine-brackish-fresh water transition with comments on the systematics and ecology of the most common diatoms. Diatom Research 7 (1), 157–194.

Watcham, E.P., Bentley, M.J., Hodgson, D.A., Roberts, S.J., Fretwell, P.T., Lloyd, J.M., Larter, R.D., Whitehouse, P.L., Leng, M.J., Monien, P., Moreton, S.G., 2011. A new relative sea level curve for the south Shetland Islands, Antarctica. Quaternary Science Reviews 30, 3152–3170.

Wetzel, R.G., 2001. Limnology: Lake and River Ecosystems. Academic Press, San Diego.

Whitaker, T.M., Richardson, M.G., 1980. Morphology and chemical-composition of a natural-population of an ice-associated Antarctic diatom Navicula-Glaciei. Journal of Phycology 16, 250–257.

Willmott, V., Domack, E.W., Canals, M., Brachfeld, S., 2006. A high resolution relative paleointensity record from the Gerlache-Boyd paleo-ice stream region, northern Antarctic Peninsula. Quaternary Research 66, 1–11.

Wright, H.E., 1967. A square-rod piston sampler for lake sediments. Journal of Sedimentary Petrology 37, 976.

Wright, S.W., Jeffrey, S.W., Mantoura, R.F.C., Llewellyn, C.A., Bjornland, T., Repeta, D., Welschmeyer, N., 1991. Improved HPLC method for the analysis of chlorophylls and carotenoids from marine-Phytoplankton. Marine Ecology-Progress Series 77, 183–196.

Zale, R., 1994a. Changes in size of the Hope Bay Adelie penguin Rookery as inferred from lake Boeckella sediment. Ecography 17, 297–304.

Zale, R., 1994b. C-14 age corrections in Antarctic lake-sediments inferred from geochemistry. Radiocarbon 36, 173–185.

Zale, R., Karlen, W., 1989. Lake sediment cores from the Antarctic Peninsula and surrounding islands. Geografiska Annaler Series A – Physical Geography 71, 211–220.

Zeeb, B.A., Smol, J.P., 2001. Chrysophyte scales and cysts (Chapter 9). In: Smol, J.P., Birks, H.J.B., Last, W.M. (Eds.), Tracking Environmental Change Using Lake Sediments. Terrestrial, Algal and Siliceous Indicators, vol. 3. Kluwer Academic Publishers, Dordrecht, pp. 203–223.